

# Value-Function-based Sequential Minimization for Bi-level Optimization

Risheng Liu, *Member, IEEE*, Xuan Liu, Shangzhi Zeng, Jin Zhang, and Yixuan Zhang

**Abstract**—Gradient-based Bi-Level Optimization (BLO) methods have been widely applied to handle modern learning tasks. However, most existing strategies are theoretically designed based on restrictive assumptions (e.g., convexity of the lower-level sub-problem), and computationally not applicable for high-dimensional tasks. Moreover, there are almost no gradient-based methods able to solve BLO in those challenging scenarios, such as BLO with functional constraints and pessimistic BLO. In this work, by reformulating BLO into approximated single-level problems, we provide a new algorithm, named Bi-level Value-Function-based Sequential Minimization (BVFSM), to address the above issues. Specifically, BVFSM constructs a series of value-function-based approximations, and thus avoids repeated calculations of recurrent gradient and Hessian inverse required by existing approaches, time-consuming especially for high-dimensional tasks. We also extend BVFSM to address BLO with additional functional constraints. More importantly, BVFSM can be used for the challenging pessimistic BLO, which has never been properly solved before. In theory, we prove the convergence of BVFSM on these types of BLO, in which the restrictive lower-level convexity assumption is completely discarded. To our best knowledge, this is the first gradient-based algorithm that can solve different kinds of BLO (e.g., optimistic, pessimistic, and with constraints) with solid convergence guarantees. Extensive experiments verify the theoretical investigations and demonstrate our superiority on various real-world applications.

**Index Terms**—Bi-level optimization, gradient-based method, value-function, sequential minimization, hyper-parameter optimization.

## 1 INTRODUCTION

CURRENTLY, a number of important machine learning and deep learning tasks can be captured by hierarchical models, such as hyper-parameter optimization [1], [2], [3], [4], neural architecture search [5], [6], [7], meta learning [8], [9], [10], Generative Adversarial Networks (GAN) [11], [12], reinforcement learning [13], image processing [14], [15], [16], [17], and so on. In general, these hierarchical models can be formulated as the following Bi-Level Optimization (BLO) problem [18], [19], [20]:

$$\min_{\mathbf{x} \in \mathcal{X}} F(\mathbf{x}, \mathbf{y}), \quad \text{s.t. } \mathbf{y} \in \mathcal{S}(\mathbf{x}) := \arg \min_{\mathbf{y}} f(\mathbf{x}, \mathbf{y}), \quad (1)$$

where  $\mathbf{x} \in \mathcal{X}$  is the Upper-Level (UL) variable,  $\mathbf{y} \in \mathbb{R}^n$  is the Lower-Level (LL) variable, the UL objective  $F(\mathbf{x}, \mathbf{y}) : \mathcal{X} \times \mathbb{R}^n \rightarrow \mathbb{R}$  and the LL objective  $f(\mathbf{x}, \mathbf{y}) : \mathbb{R}^m \times \mathbb{R}^n \rightarrow \mathbb{R}$ , are continuously differentiable and jointly continuous functions, and the UL constraint  $\mathcal{X} \subset \mathbb{R}^m$  is a compact set. Nevertheless, the model in Eq. (1) cannot be solved directly. Some existing works only consider the case that the LL solution set  $\mathcal{S}(\mathbf{x})$  is a singleton. However, since this may not be satisfied and

$\mathbf{y} \in \mathcal{S}(\mathbf{x})$  may not be unique, Eq. (1) is not a rigorous BLO model in mathematics, and thus we use the quotation marks around “min” to denote the slightly imprecise definition of the UL objective [18], [21].

Strictly, people usually focus on an extreme situation of the BLO model, i.e., the optimistic BLO [18]:

$$\min_{\mathbf{x} \in \mathcal{X}} \min_{\mathbf{y} \in \mathbb{R}^n} F(\mathbf{x}, \mathbf{y}), \quad \text{s.t. } \mathbf{y} \in \mathcal{S}(\mathbf{x}). \quad (2)$$

It can be found from the above expression that in optimistic BLO,  $\mathbf{x}$  and  $\mathbf{y}$  are in a cooperative relationship, aiming to minimize  $F(\mathbf{x}, \mathbf{y})$  at the same time. Therefore, it can be applied to a variety of learning and vision tasks, such as hyper-parameter optimization, meta learning, and so on. Sometimes we also need to study BLO problems with inequality constraints on the UL or LL for capturing constraints in real tasks. Another situation one can consider is the pessimistic BLO, which changes the  $\min_{\mathbf{y} \in \mathbb{R}^n}$  in Eq. (2) into  $\max_{\mathbf{y} \in \mathbb{R}^n}$  [18]. In the pessimistic case,  $\mathbf{x}$  and  $\mathbf{y}$  are in an adversarial relationship, and hence solving pessimistic BLO can be applied to adversarial learning and GAN.

Actually, BLO is challenging to solve, because in the hierarchical structure, we need to solve  $\mathcal{S}(\mathbf{x})$  governed by the fixed  $\mathbf{x}$ , and select an appropriate  $\mathbf{y}$  from  $\mathcal{S}(\mathbf{x})$  to optimize the UL  $F(\mathbf{x}, \mathbf{y})$ , making  $\mathbf{x}$  and  $\mathbf{y}$  intricately dependent of each other, especially when  $\mathcal{S}(\mathbf{x})$  is not a singleton [22]. In classical optimization, KKT condition is utilized to characterize the problem, but this method is not applicable to machine learning tasks of large scale due to the use of too many multipliers [23], [24]. In machine learning community, a class of mainstream and popular methods are gradient-based methods, divided into Explicit Gradient-Based Methods (EGBMs) [2], [8], [25], [26], [5] and Implicit Gradient-Based Methods (IGBMs) [27], [9], [28], according

- R. Liu and X. Liu are with the DUT-RU International School of Information Science & Engineering, Dalian University of Technology, and the Key Laboratory for Ubiquitous Network and Service Software of Liaoning Province, Dalian, Liaoning, China. R. Liu is also with the Pazhou Lab, Guangzhou, Guangdong, China. E-mail: rslu@dlut.edu.cn, liuxuan\_16@126.com.
- S. Zeng is with the Department of Mathematics and Statistics, University of Victoria, Victoria, B.C., Canada. E-mail: zengshangzhi@gmail.com.
- J. Zhang is with the Department of Mathematics, SUSTech International Center for Mathematics, Southern University of Science and Technology, and National Center for Applied Mathematics Shenzhen, Shenzhen, Guangdong, China. (Corresponding author, E-mail: zhangj9@sustech.edu.cn.)
- Y. Zhang is with the Department of Mathematics, Southern University of Science and Technology, Shenzhen, Guangdong, China. E-mail: zhangyx2020@mail.sustech.edu.cn.

Manuscript received April 19, 2005; revised August 26, 2015.

to divergent ideas of calculating the gradient needed for implementing gradient descent. EGBMs implement this process via unrolled differentiation, and IGBMs use the implicit function theorem to obtain the gradient. Both of them usually deal with the problem where the LL solution set  $\mathcal{S}(\mathbf{x})$  is a singleton, which is a quite restrictive condition in real application tasks. In dealing with this, Liu et al. [29], [30] proposed Bi-level Descent Aggregation (BDA) as a new EGBM, which removes this assumption and solves the model from the perspective of optimistic BLO.

Nevertheless, there still exists a bottleneck hard to break through, that the LL problems in real learning tasks are usually too complex for EGBMs and IGBMs. In theory, all of the EGBMs and IGBMs require the convexity of the LL problem, or the Lower-Level Convexity, denoted as LLC for short, which is a strict condition and not satisfied in many complicated real-world tasks. For example, since the layer of chosen network is usually greater than one, LLC is not satisfied, and thus the convergence of these methods cannot be guaranteed. What's more, as for computation, EGBMs using unrolled differentiation request large time and space complexity, while IGBMs need to approximate the inverse of a matrix, also with high computational cost, especially when the LL variable  $\mathbf{y}$  is of large scale, which means the dimension of  $\mathbf{y}$  is large, generating matrices and vectors of high dimension during the calculating procedure. Besides, it has been rarely discussed how to handle machine learning tasks by solving an optimization problem with functional constraints on the UL and LL, or by solving a pessimistic BLO. However, these problems are worth discussing, because pessimistic BLO can be used to capture min-max bi-level structures, which is suitable for GAN and so on, and optimization problems with constraints can be used to represent learning tasks more accurately. Unfortunately, existing methods, all EGBMs and IGBMs, are not able to handle these problems.

To address the above limitations of existing methods, in this work, we propose a novel framework, named Bi-level Value-Function-based Sequential Minimization (BVFSM)<sup>1</sup>. To be specific, we start with reformulating BLO into a simple bi-level optimization problem by the value-function [31], [32] of UL objective. After that, we further transform it into a single-level optimization problem with an inequality constraint through the value-function of LL objective. Then, by using the smoothing technique via regularization and adding the constraint into the objective by an auxiliary function of penalty or barrier, eventually the original problem can be transformed into a sequence of unconstrained differentiable single-level problems, which can be solved by gradient descent. Thanks to the re-characterization via the value-function of LL problem, BVFSM can be applied under more relaxed conditions, and simultaneously, our computational cost is the least to implement the algorithm. Specifically, we prove that the solutions of the sequence of approximate sub-problems converge to the true solution of the original BLO without the restrictive LLC assumption as before. In addition, BVFSM avoids solving an unrolled dynamic system by recurrent gradient or approximating the inverse of Hessian during each iteration like existing methods. Instead, we only

need to calculate the first-order gradient in each iteration, and thus require less time and space complexity than EGBMs and IGBMs, especially for complex high-dimensional BLO. We illustrate the efficiency of BVFSM over existing methods through complexity analysis in theory and various experimental results in reality. Also, BVFSM can be extended to more complicated and challenging scenarios, namely, BLO with functional constraints and pessimistic BLO problems. We regard pessimistic BLO as a new viewpoint to deal with learning tasks, which has not been solved by gradient-based methods before to our best knowledge. Specially, we use the experiment of GAN as an example to illustrate the application of our method for solving pessimistic BLO. We summarize our contributions as follows.

- By reformulating the original BLO as an approximated single-level problem based on the value-function, BVFSM establishes a competently new sequential minimization algorithmic framework, which not only can be used to address optimistic BLO, but also has the ability to handle BLO in other more challenging scenarios (i.e., with functional constraints and pessimistic), which have seldom been discussed.
- Theoretically, we rigorously analyze the convergence behaviors of BVFSM on all types of BLO mentioned above. Our theoretical investigations successfully remove the restrictive LLC condition, required in most existing works but actually too ambitious to satisfy in real-world applications.
- Computationally, as BVFSM provides a value-function-based reformulation for BLO, it completely avoids the repeated calculations of recurrent gradient and Hessian inverse, caused by existing approaches. Indeed, these time-consuming calculations are the core bottleneck for solving high-dimensional BLO.
- Experimentally, we conduct extensive experiments to verify our theoretical findings and demonstrate the superiority of BVFSM on various learning tasks. Especially, by formulating and solving GAN by BVFSM, we also show the application potential of our solution strategy on pessimistic BLO for complex learning problems.

## 2 RELATED WORKS

As aforementioned, BLO is challenging to solve due to its nested structures between UL and LL. Early methods can only handle models with not too many hyper-parameters. For example, to find appropriate parameters, the standard method is to use random search [33] through randomly sampling, or to use Bayesian optimization [34]. However, in real learning tasks, the dimension of hyper-parameters is very large, which early methods cannot deal with, so gradient-based methods are proposed. Here we first put forward a unified form of gradient-based methods, and then discuss the existing methods for further comparing them with our proposed method to show our superiority.

Existing gradient-based methods mainly focus on the optimistic BLO only, so we use the scenario of optimistic BLO to illustrate our algorithmic framework clearly, while in Section 3.4, we will discuss how to use our method to solve pessimistic BLO. For optimistic BLO, it can be found from

1. A preliminary version of this work has been published in [1].

Eq. (2) that the UL variable  $\mathbf{x}$  and LL variable  $\mathbf{y}$  will effect each other in a nested relationship. To address this issue, one can transform it into the following form, where  $\varphi(\mathbf{x})$  is the value-function of the sub-problem,

$$\min_{\mathbf{x} \in \mathcal{X}} \varphi(\mathbf{x}), \quad \varphi(\mathbf{x}) := \min_{\mathbf{y}} \left\{ F(\mathbf{x}, \mathbf{y}) : \mathbf{y} \in \mathcal{S}(\mathbf{x}) \right\}. \quad (3)$$

For a fixed  $\mathbf{x}$ , this sub-problem for solving  $\varphi(\mathbf{x})$  is an inner simple BLO task, as it is only about one variable  $\mathbf{y}$ , with  $\mathbf{x}$  as a parameter. Then, we hope to  $\min \varphi(\mathbf{x})$  through gradient descent. However, as a value-function,  $\varphi(\mathbf{x})$  is non-smooth, non-convex, and even with jumps, thus ill-conditioned, so we use a smooth function to approximate  $\varphi(\mathbf{x})$  and obtain  $\frac{\partial \varphi(\mathbf{x})}{\partial \mathbf{x}}$ . Existing methods can be classified into two categories according to divergent ways to calculate  $\frac{\partial \varphi(\mathbf{x})}{\partial \mathbf{x}}$  [20], [35], [36], i.e., Explicit Gradient-Based Methods (EGBMs), which derives the gradient by Automatic Differentiation (AD), and Implicit Gradient-Based Methods (IGBMs), which apply the implicit function theorem to deal with the optimality conditions of LL problems.

Note that both EGBMs and IGBMs require  $\mathbf{y} \in \mathcal{S}(\mathbf{x})$  to be unique (except BDA), denoted as  $\mathbf{y}^*(\mathbf{x})$ , while for BDA, by integrating information from both the UL and LL sub-problem,  $\mathbf{y}_T(\mathbf{x})$  is obtained by iterations to approach the appropriate  $\mathbf{y}^*(\mathbf{x})$ . Hence,  $\varphi(\mathbf{x}) = F(\mathbf{x}, \mathbf{y}^*(\mathbf{x}))$ , and therefore by the chain rule, the approximated  $\frac{\partial \varphi(\mathbf{x})}{\partial \mathbf{x}}$  is split into direct and indirect gradients of  $\mathbf{x}$ ,

$$\frac{\partial \varphi(\mathbf{x})}{\partial \mathbf{x}} = \frac{\partial F(\mathbf{x}, \mathbf{y}^*(\mathbf{x}))}{\partial \mathbf{x}} + G(\mathbf{x}), \quad (4)$$

where  $\frac{\partial F(\mathbf{x}, \mathbf{y})}{\partial \mathbf{x}}$  is the direct gradient and  $G(\mathbf{x})$  is the indirect gradient,  $G(\mathbf{x}) = \left( \frac{\partial \mathbf{y}^*(\mathbf{x})}{\partial \mathbf{x}} \right)^\top \frac{\partial F(\mathbf{x}, \mathbf{y}^*)}{\partial \mathbf{y}}$ . Then we need to compute  $G(\mathbf{x})$ , in other words, the value of  $\frac{\partial \mathbf{y}^*(\mathbf{x})}{\partial \mathbf{x}}$ .

**Explicit Gradient-Based Methods (EGBMs).** Maclaurin et al. [25] and Franceschi et al. [2], [8] first proposed Reverse Hyper-Gradient (RHG) and Forward Hyper-Gradient (FHG) respectively, to implement a dynamic system, under the LLC assumption. Given an initial point  $\mathbf{y}_0$ , denote the iteration process to approach  $\mathbf{y}^*(\mathbf{x})$  as  $\mathbf{y}_{t+1}(\mathbf{x}) = \Phi_t(\mathbf{x}, \mathbf{y}_t(\mathbf{x}))$ ,  $t = 0, 1, \dots, T-1$ , where  $\Phi$  is a smooth mapping performed to solve  $\mathbf{y}_T(\mathbf{x})$  and  $T$  is the number of iterations. In particular, for example, if the process is gradient descent,  $\Phi_t(\mathbf{x}, \mathbf{y}_t(\mathbf{x})) = \mathbf{y}_t(\mathbf{x}) - s_t \frac{\partial f(\mathbf{x}, \mathbf{y}_t(\mathbf{x}))}{\partial \mathbf{y}}$ , where  $s_t > 0$  is the corresponding step size. Then  $\varphi(\mathbf{x})$  in Eq. (3) can be approximated by  $\varphi(\mathbf{x}) \approx \varphi_T(\mathbf{x}) = F(\mathbf{x}, \mathbf{y}_T(\mathbf{x}))$ . As  $T$  increases,  $\varphi_T(\mathbf{x})$  approaches  $\varphi(\mathbf{x})$  generally, and a sequence of unconstrained minimization problems is obtained. Thus, gradient-based methods can be regarded as a kind of sequential-minimization-type scheme [37]. From the chain rule, we have  $\frac{\partial \mathbf{y}_t(\mathbf{x})}{\partial \mathbf{x}} = \left( \frac{\partial \Phi_{t-1}(\mathbf{x}, \mathbf{y}_{t-1})}{\partial \mathbf{y}_{t-1}} \right)^\top \frac{\partial \mathbf{y}_{t-1}(\mathbf{x})}{\partial \mathbf{x}} + \frac{\partial \Phi_{t-1}(\mathbf{x}, \mathbf{y}_{t-1})}{\partial \mathbf{x}}$ , and  $\frac{\partial \mathbf{y}_T(\mathbf{x})}{\partial \mathbf{x}}$  can be obtained from this unrolled procedure. However, FHG and RHG require calculating the gradient of  $\mathbf{x}$  composed of the first-order condition of LL problem by AD during the entire trajectory, so the computational cost owing to the time and space complexity is very high. In dealing with this, Shaban et al. [26] proposed Truncated Reverse Hyper-Gradient (TRHG) to truncate the iteration, and thus TRHG only needs to store the last  $I$  iterations, reducing the computational load. Nevertheless, it additionally requires  $f$

to be strongly convex, and the truncated path length is hard to determine. Another method Liu et al. [5] tried is to use difference of vectors to approximate the gradient, but the accuracy of using difference is not promised and there is no theoretical guarantee for this method. On the other hand, from the viewpoint of theory, for more relaxed conditions, Liu et al. [29], [30] proposed Bi-level Descent Aggregation (BDA) to remove the assumption that the LL solution set is a singleton, which is a simplification of real-world problems. Specifically, BDA uses information from both the UL and the LL problem as an aggregation during iterations. However, the obstacle of LLC and computational cost still exists.

**Implicit Gradient-Based Methods (IGBMs).** IGBMs or implicit differentiation [27], [9], [28], can be applied to obtain  $\frac{\partial \mathbf{y}^*(\mathbf{x})}{\partial \mathbf{x}}$  under the LLC assumption. If  $\frac{\partial^2 f(\mathbf{x}, \mathbf{y}^*(\mathbf{x}))}{\partial \mathbf{y} \partial \mathbf{y}}$  is assumed to be invertible in advance as an additional condition, by using the implicit function theorem on the optimality condition  $\frac{\partial f(\mathbf{x}, \mathbf{y}^*(\mathbf{x}))}{\partial \mathbf{y}} = 0$ , the LL problem is replaced with an implicit equation, and then  $\frac{\partial \mathbf{y}^*(\mathbf{x})}{\partial \mathbf{x}} = - \left( \frac{\partial^2 f(\mathbf{x}, \mathbf{y}^*(\mathbf{x}))}{\partial \mathbf{y} \partial \mathbf{y}} \right)^{-1} \frac{\partial^2 f(\mathbf{x}, \mathbf{y}^*(\mathbf{x}))}{\partial \mathbf{y} \partial \mathbf{x}}$ . Unlike EGBMs relying on the first-order condition during the entire trajectory, IGBMs only depends on the first-order condition once, which decouples the computational burden from the solution trajectory of the LL problem, but this leads to repeated computation of the inverse of Hessian matrix, which is still a heavy burden. In dealing with this, to avoid direct inverse calculation, the Conjugate Gradient (CG) method [27], [9] changes it into solving a linear system, and Neumann method [28] uses the Neumann series to calculate the Hessian inverse. However, after using these methods, the computational requirements are reduced but still large, because the burden of computing the inverse of matrix changes into computing Hessian-vector products. Additionally, the accuracy of solving a linear system highly depends on its condition number [38], and ill condition may result in numerical instabilities. A large quadratic term is added on the LL objective to eliminate the ill-condition in [9], but this approach may change the solution set greatly.

As discussed above, EGBMs and IGBMs need repeated calculations of recurrent gradient or Hessian inverse, leading to high time and space complexity in numerical computation, and require the LLC assumption in theory. Actually, when the dimension of  $\mathbf{y}$  is very large, which happens in practical problems usually, the computational burden of massively computing the products of matrices and vectors might be too heavy to carry. In addition, the LLC assumption is also not suitable for most complex real-world tasks.

### 3 THE PROPOSED ALGORITHM

In this section, we illustrate our algorithmic framework, named Bi-level Value-Function-based Sequential Minimization (BVFSM). Our method also follows the idea of constructing a sequence of unconstrained minimization problems to approximate the original bi-level problem, but different from existing methods, BVFSM uses the re-characterization via the value-function of the LL problem. Thanks to this, our algorithm is able to handle problems with complicated non-convex high-dimensional LL, which existing methods are not able to deal with.

### 3.1 Value-Function-based Single-level Reformulation

Our BVFSM designs a sequence of single-level unconstrained minimization problems to approximate the original problem through a value-function-based reformulation. We first present this procedure under the optimistic BLO case. Recall the original optimistic BLO in Eq. (2) has been transformed into Eq. (3), and we hope to compute  $G(\mathbf{x})$  in Eq. (4). Note that the difficulty of computing  $\frac{\partial \varphi(\mathbf{x})}{\partial \mathbf{x}}$  comes from the ill-condition of  $\varphi(\mathbf{x})$ , owing to the nested structure of the bi-level sub-problem for solving  $\varphi(\mathbf{x})$ . Hence, we hope to transform it into a single-level problem, and introduce the value-function of the LL problem  $f^*(\mathbf{x}) := \min_{\mathbf{y}} f(\mathbf{x}, \mathbf{y})$ . Then the problem can be reformulated as

$$\varphi(\mathbf{x}) = \min_{\mathbf{y}} \left\{ F(\mathbf{x}, \mathbf{y}) : f(\mathbf{x}, \mathbf{y}) \leq f^*(\mathbf{x}) \right\}. \quad (5)$$

However, the inequality constraint  $f(\mathbf{x}, \mathbf{y}) \leq f^*(\mathbf{x})$  is still ill-posed, because it does not satisfy any standard regularity condition, and  $f^*(\mathbf{x})$  is non-smooth. In dealing with such difficulty, we approximate the value-function  $f^*(\mathbf{x})$  with a regularization term:

$$f_{\mu}^*(\mathbf{x}) = \min_{\mathbf{y}} \left\{ f(\mathbf{x}, \mathbf{y}) + \frac{\mu}{2} \|\mathbf{y}\|^2 \right\}, \quad (6)$$

where  $\frac{\mu}{2} \|\mathbf{y}\|^2$  ( $\mu > 0$ ) improves the computational stability.

We further add an auxiliary function of the inequality constraints to the objective, and obtain

$$\varphi_{\mu, \theta, \sigma}(\mathbf{x}) = \min_{\mathbf{y}} \left\{ F(\mathbf{x}, \mathbf{y}) + P_{\sigma}(f(\mathbf{x}, \mathbf{y}) - f_{\mu}^*(\mathbf{x})) + \frac{\theta}{2} \|\mathbf{y}\|^2 \right\}, \quad (7)$$

where  $(\mu, \theta, \sigma) > 0$ , the regularization term  $\frac{\theta}{2} \|\mathbf{y}\|^2$  is for improving the computational stability, and  $P_{\sigma} : \mathbb{R} \rightarrow \mathbb{R}$  (here  $\mathbb{R}$  denotes  $\mathbb{R} \cup \{\infty\}$ ) is the selected auxiliary function for the sequential unconstrained minimization method with parameter  $\sigma$ , which will be discussed in detail next. This reformulation changes the constrained problem Eq. (5) into a sequence of unconstrained problems Eq. (7) under different parameters.

The sequential unconstrained minimization method is mainly used for solving constrained nonlinear programming by changing the problem into a sequence of unconstrained minimization problems [37], [39], [40]. To be specific, we add to the objective a selected auxiliary function of the constraints with a sequence of parameters, and obtain a series of unconstrained problems. The convergence of parameters makes the sequential unconstrained problems converge to the original constrained problem, leading to the convergence of the solution. Based on the property of auxiliary functions, they are divided mainly into two types, barrier functions and penalty functions [41], [42]. Here we put forward the definition of barrier or penalty functions.

**Definition 1** A continuous, differentiable, and non-decreasing function  $\rho : \mathbb{R} \rightarrow \mathbb{R}$  is called a standard barrier function if  $\rho(\omega; \sigma)$  satisfies  $\rho(\omega; \sigma) \geq 0$  and  $\lim_{\sigma \rightarrow 0} \rho(\omega; \sigma) = 0$ , when  $\omega < 0$ ; and  $\rho(\omega; \sigma) \rightarrow \infty$  when  $\omega \rightarrow 0$ . It is called a standard penalty function if it satisfies  $\rho(\omega; \sigma) = 0$  when  $\omega \leq 0$ ; and  $\rho(\omega; \sigma) > 0$  and  $\lim_{\sigma \rightarrow 0} \rho(\omega; \sigma) = \infty$  when  $\omega > 0$ . Here  $\sigma > 0$  is the barrier or penalty parameter. In addition, if  $\rho(\omega; \sigma^{(1)})$  is a standard barrier function,  $\rho(\omega - \sigma^{(2)}; \sigma^{(1)})$  ( $\sigma^{(1)}, \sigma^{(2)} > 0$ ) is called a modified barrier function.

For the simplicity of expression later, we denote the function  $P_{\sigma}$  in Eq. (7) to be

$$P_{\sigma}(\omega) := \begin{cases} \rho(\omega; \sigma), & \text{if } \rho \text{ is a penalty} \\ & \text{or standard barrier function,} \\ \rho(\omega - \sigma^{(2)}; \sigma^{(1)}), & \text{if } \rho \text{ is a modified barrier function.} \end{cases} \quad (8)$$

Here for a modified barrier function,  $\sigma^{(2)} > 0$  is to guarantee that in Eq. (7),  $f(\mathbf{x}, \mathbf{y}) - f_{\mu}^*(\mathbf{x}) - \sigma^{(2)} < 0$ , and the barrier function is well-defined.

Classical examples of auxiliary functions are the quadratic penalty function, inverse barrier function and log barrier function [43], [42]. There are also some other popular examples, such as the polynomial penalty function [41] and truncated log barrier function [44]. These available standard penalty and barrier functions are listed in Table 1. Note that we want the smoothness of  $\varphi_{\mu, \theta, \sigma}(\mathbf{x})$ , and will calculate the gradient of  $P_{\sigma}$  afterwards, so we choose smooth auxiliary functions, instead of non-smooth exact penalty functions.

TABLE 1  
Some of the available standard penalty and barrier functions.

Penalty functions	
Quadratic	$\rho(\omega; \sigma) = \frac{1}{2\sigma} (\omega^+)^2$ , where $\omega^+ = \max\{\omega, 0\}$
Polynomial	$\rho(\omega; \sigma) = \frac{1}{q\sigma} (\omega^+)^q$ , where $q$ is a positive integer chosen such that $\rho(\omega; \sigma)$ is differentiable
Barrier functions	
Inverse	$\rho(\omega; \sigma) = \begin{cases} -\frac{\sigma}{\omega}, & \omega < 0 \\ \infty, & \omega \geq 0 \end{cases}$
Truncated Log	$\rho(\omega; \sigma) = \begin{cases} -\sigma (\log(-\omega) + \beta_1), & -\kappa \leq \omega < 0 \\ -\sigma \left( \beta_2 + \frac{\beta_3}{\omega^2} + \frac{\beta_4}{\omega} \right), & \omega < -\kappa \\ \infty, & \omega \geq 0 \end{cases}$ where $0 < \kappa \leq 1$ , $\beta_1, \beta_2, \beta_3, \beta_4$ are chosen such that $\rho(\omega; \sigma) \geq 0$ and is twice differentiable

### 3.2 Sequential Minimization Strategy

From the discussion above, we then hope to solve

$$\min_{\mathbf{x} \in \mathcal{X}} \varphi_{\mu, \theta, \sigma}(\mathbf{x}), \quad (9)$$

with  $\varphi_{\mu, \theta, \sigma}(\mathbf{x})$  in Eq. (7). First denote

$$\mathbf{z}_{\mu}^*(\mathbf{x}) = \argmin_{\mathbf{y}} \left\{ f(\mathbf{x}, \mathbf{y}) + \frac{\mu}{2} \|\mathbf{y}\|^2 \right\}, \quad (10)$$

and

$$\mathbf{y}_{\mu, \theta, \sigma}^*(\mathbf{x}) = \argmin_{\mathbf{y}} \left\{ F(\mathbf{x}, \mathbf{y}) + P_{\sigma}(f(\mathbf{x}, \mathbf{y}) - f_{\mu}^*(\mathbf{x})) + \frac{\theta}{2} \|\mathbf{y}\|^2 \right\}. \quad (11)$$

The following proposition gives the smoothness of  $\varphi_{\mu, \theta, \sigma}(\mathbf{x})$  and the formula for computing  $\frac{\partial \varphi_{\mu, \theta, \sigma}(\mathbf{x})}{\partial \mathbf{x}^2}$  or  $G(\mathbf{x})$ , which serves as the ground for our algorithm<sup>2</sup>.

**Proposition 1 (Calculation of  $G(\mathbf{x})$ )** Suppose  $F(\mathbf{x}, \mathbf{y})$  and  $f(\mathbf{x}, \mathbf{y})$  are bounded below and continuously differentiable. Given

2. The convergence analysis of  $\varphi_{\mu, \theta, \sigma}(\mathbf{x}) \rightarrow \varphi(\mathbf{x})$  will be discussed in Section 4.1.

$\mathbf{x} \in \mathcal{X}$  and  $\mu, \theta, \sigma > 0$ , when  $\mathbf{z}_\mu^*(\mathbf{x})$  and  $\mathbf{y}_{\mu,\theta,\sigma}^*(\mathbf{x})$  are unique, then  $\varphi_{\mu,\theta,\sigma}(\mathbf{x})$  is differentiable and

$$G(\mathbf{x}) = \frac{\partial P_\sigma(f(\mathbf{x}, \mathbf{y}) - f_\mu^*(\mathbf{x}))}{\partial \mathbf{x}} \Big|_{\mathbf{y}=\mathbf{y}_{\mu,\theta,\sigma}^*(\mathbf{x})}, \quad (12)$$

where  $f_\mu^*(\mathbf{x}) = f(\mathbf{x}, \mathbf{z}_\mu^*(\mathbf{x})) + \frac{\mu}{2} \|\mathbf{z}_\mu^*(\mathbf{x})\|^2$ , and  $\frac{\partial f_\mu^*(\mathbf{x})}{\partial \mathbf{x}} = \frac{\partial f(\mathbf{x}, \mathbf{y})}{\partial \mathbf{x}} \Big|_{\mathbf{y}=\mathbf{z}_\mu^*(\mathbf{x})}$ .

*Proof:* We first prove that for any  $\bar{\mathbf{x}} \in \mathcal{X}$ ,  $f(\mathbf{x}, \mathbf{y}) + \frac{\mu}{2} \|\mathbf{y}\|^2$  is level-bounded in  $\mathbf{y}$  locally uniformly in  $\bar{\mathbf{x}} \in \mathcal{X}$  (see [29, Definition 3]), i.e., for any  $c \in \mathbb{R}$ , there exist  $\delta > 0$  and a bounded set  $\mathcal{B} \in \mathbb{R}^n$ , such that

$$\left\{ \mathbf{y} \in \mathbb{R}^n \mid f(\mathbf{x}, \mathbf{y}) + \frac{\mu}{2} \|\mathbf{y}\|^2 \leq c \right\} \subseteq \mathcal{B},$$

for all  $\mathbf{x} \in \mathcal{B}_\delta(\bar{\mathbf{x}}) \cap \mathcal{X}$ . Assume by contradiction that the above does not hold. Then there exist sequences  $\{\mathbf{x}_k\}$  and  $\{\mathbf{y}_k\}$  satisfying  $\mathbf{x}_k \rightarrow \bar{\mathbf{x}}$  and  $\|\mathbf{y}_k\| \rightarrow +\infty$ , such that  $f(\mathbf{x}_k, \mathbf{y}_k) + \frac{\mu}{2} \|\mathbf{y}_k\|^2 \leq c$ . As  $f(\mathbf{x}, \mathbf{y})$  is bounded below, then  $\|\mathbf{y}_k\| \rightarrow \infty$  implies  $f(\mathbf{x}_k, \mathbf{y}_k) + \frac{\mu}{2} \|\mathbf{y}_k\|^2 \rightarrow \infty$ , which contradicts with  $f(\mathbf{x}_k, \mathbf{y}_k) + \frac{\mu}{2} \|\mathbf{y}_k\|^2 \leq c$  and  $c \in \mathbb{R}$ .

Hence, from the arbitrariness of  $\bar{\mathbf{x}}$ , we have  $f(\mathbf{x}, \mathbf{y}) + \frac{\mu}{2} \|\mathbf{y}\|^2$  is level-bounded in  $\mathbf{y}$  locally uniformly in  $\mathbf{x} \in \mathcal{X}$ , and then the inf-compactness condition in [45, Theorem 4.13] holds for  $f(\mathbf{x}, \mathbf{y}) + \frac{\mu}{2} \|\mathbf{y}\|^2$ . Since  $\operatorname{argmin}_{\mathbf{y} \in \mathbb{R}^n} \{f(\mathbf{x}, \mathbf{y}) + \frac{\mu}{2} \|\mathbf{y}\|^2\}$  is a singleton, it follows from [45, Theorem 4.13, Remark 4.14] that

$$\frac{\partial f_\mu^*(\mathbf{x})}{\partial \mathbf{x}} = \frac{\partial (f(\mathbf{x}, \mathbf{y}) + \frac{\mu}{2} \|\mathbf{y}\|^2)}{\partial \mathbf{x}} \Big|_{\mathbf{y}=\mathbf{z}_\mu^*(\mathbf{x})} = \frac{\partial f(\mathbf{x}, \mathbf{y})}{\partial \mathbf{x}} \Big|_{\mathbf{y}=\mathbf{z}_\mu^*(\mathbf{x})}.$$

Next, from definitions of penalty and barrier functions (see Definition 1), we have  $\rho(\omega; \sigma) \geq 0$  for any  $\omega$ , and thus  $P_\sigma(\omega) \geq 0$  holds. Then, since  $F(\mathbf{x}, \mathbf{y})$  is assumed to be bounded below, similar to  $f(\mathbf{x}, \mathbf{y}) + \frac{\mu}{2} \|\mathbf{y}\|^2$ , for

$$F(\mathbf{x}, \mathbf{y}) + P_\sigma(f(\mathbf{x}, \mathbf{y}) - f_\mu^*(\mathbf{x})) + \frac{\theta}{2} \|\mathbf{y}\|^2,$$

the inf-compactness condition in [45, Theorem 4.13] also holds. Combining with the fact that

$$\operatorname{argmin}_{\mathbf{y} \in \mathbb{R}^n} \left\{ F(\mathbf{x}, \mathbf{y}) + P_\sigma(f(\mathbf{x}, \mathbf{y}) - f_\mu^*(\mathbf{x})) + \frac{\theta}{2} \|\mathbf{y}\|^2 \right\}$$

is a singleton, [45, Theorem 4.13, Remark 4.14] shows that

$$\begin{aligned} & \frac{\partial \varphi_{\mu,\theta,\sigma}(\mathbf{x})}{\partial \mathbf{x}} \\ &= \frac{\partial (F(\mathbf{x}, \mathbf{y}) + P_\sigma(f(\mathbf{x}, \mathbf{y}) - f_\mu^*(\mathbf{x})) + \frac{\theta}{2} \|\mathbf{y}\|^2)}{\partial \mathbf{x}} \Big|_{\mathbf{y}=\mathbf{y}_{\mu,\theta,\sigma}^*(\mathbf{x})} \\ &= \left( \frac{\partial F(\mathbf{x}, \mathbf{y})}{\partial \mathbf{x}} + \frac{\partial P_\sigma(f(\mathbf{x}, \mathbf{y}) - f_\mu^*(\mathbf{x}))}{\partial \mathbf{x}} \right) \Big|_{\mathbf{y}=\mathbf{y}_{\mu,\theta,\sigma}^*(\mathbf{x})}. \end{aligned}$$

Therefore, the conclusion in Eq. (12) follows immediately.  $\square$

Proposition 1 serves as the foundation for our algorithmic framework. Denote  $\varphi_k(\mathbf{x}) := \varphi_{\mu_k, \theta_k, \sigma_k}(\mathbf{x})$ . Next, we will illustrate the implementation at the  $k$ -th step of the outer loop and the  $l$ -th step of the inner loop, that is, to calculate  $\frac{\partial \varphi_k(\mathbf{x}_l)}{\partial \mathbf{x}}$ , as a guide.

We first calculate  $\mathbf{z}_{\mu_k}^*(\mathbf{x}_l)$  in Eq. (10) through  $T_z$  steps of gradient descent, and denote the output as  $\mathbf{z}_{k,l}^{T_z}$ , regarded as an approximation of  $\mathbf{z}_{\mu_k}^*(\mathbf{x}_l)$ . After that, we calculate

$\mathbf{y}_{\mu_k, \theta_k, \sigma_k}^*(\mathbf{x}_l)$  in Eq. (11) through  $T_y$  steps of gradient descent, and denote the output as  $\mathbf{y}_{k,l}^{T_y}$ . Then, according to Proposition 1, we can obtain

$$\frac{\partial \varphi_k(\mathbf{x}_l)}{\partial \mathbf{x}} \approx \frac{\partial F(\mathbf{x}_l, \mathbf{y}_{k,l}^{T_y})}{\partial \mathbf{x}} + G_{k,l}, \quad (13)$$

with

$$G_{k,l} = \frac{\partial P_{\sigma_k} \left( f(\mathbf{x}_l, \mathbf{y}_{k,l}^{T_y}) - f_{k,l}^{T_z} \right)}{\partial \mathbf{x}},$$

where  $f_{k,l}^{T_z} = f(\mathbf{x}_l, \mathbf{z}_{k,l}^{T_z}) + \frac{\mu_k}{2} \|\mathbf{z}_{k,l}^{T_z}\|^2$ .

As a summary, the algorithm for solving Eq. (9) is outlined in Algorithms 1 and 2.

---

#### Algorithm 1 Our Solution Strategy for Eq. (9).

---

**Input:**  $\mathbf{x}_0, (\mu_0, \theta_0, \sigma_0)$ , step size  $\alpha > 0$ .

**Output:** The optimal UL solution  $\mathbf{x}^*$ .

- 1: **for**  $k = 0 \rightarrow K - 1$  **do**
  - 2:   Calculate  $(\mu_k, \theta_k, \sigma_k)$ .
  - 3:   **for**  $l = 0 \rightarrow L - 1$  **do**
  - 4:     Calculate  $\frac{\partial \varphi_k(\mathbf{x}_l)}{\partial \mathbf{x}}$  by Algorithm 2.
  - 5:      $\mathbf{x}_{l+1} = \operatorname{Proj}_{\mathcal{X}} \left( \mathbf{x}_l - \alpha \frac{\partial \varphi_k(\mathbf{x}_l)}{\partial \mathbf{x}} \right)$ .
  - 6:   **end for**
  - 7:    $\mathbf{x}_0 = \mathbf{x}_L$ .
  - 8: **end for**
  - 9: **return**  $\mathbf{x}^*$ .
- 

---

#### Algorithm 2 Calculation of $\frac{\partial \varphi_k(\mathbf{x}_l)}{\partial \mathbf{x}}$ .

---

**Input:**  $\mathbf{x}_l, (\mu_k, \theta_k, \sigma_k)$ .

**Output:**  $\frac{\partial \varphi_k(\mathbf{x}_l)}{\partial \mathbf{x}}$ .

- 1: Calculate  $\mathbf{z}_{k,l}^{T_z}$  as an approximation of  $\mathbf{z}_{\mu_k}^*(\mathbf{x}_l)$  by performing  $T_z$ -step gradient descent on Eq. (10).
  - 2: Calculate  $\mathbf{y}_{k,l}^{T_y}$  as an approximation of  $\mathbf{y}_{\mu_k, \theta_k, \sigma_k}^*(\mathbf{x}_l)$  by performing  $T_y$ -step gradient descent on Eq. (11).
  - 3: Calculate an approximation of  $\frac{\partial \varphi_k(\mathbf{x}_l)}{\partial \mathbf{x}}$  by Eq. (13).
- 

### 3.3 Extension for BLO with Functional Constraints

We consider the BLO with functional constraints on UL and LL problems in this subsection, which is a more general setting, and the above discussion without constraints can be extended to the case with inequality constraints.

The optimistic BLO problems in Eq. (2) with functional constraints are then

$$\begin{aligned} & \min_{\mathbf{x} \in \mathcal{X}, \mathbf{y} \in \mathbb{R}^n} F(\mathbf{x}, \mathbf{y}) \\ & \text{s.t.} \quad \begin{cases} H_j(\mathbf{x}, \mathbf{y}) \leq 0, \text{ for any } j \\ \mathbf{y} \in \mathcal{S}(\mathbf{x}) := \arg \min_{\mathbf{y}} \left\{ f(\mathbf{x}, \mathbf{y}) : h_{j'}(\mathbf{x}, \mathbf{y}) \leq 0, \text{ for any } j' \right\} \end{cases} \end{aligned}$$

where the UL constraints  $H_j(\mathbf{x}, \mathbf{y}) : \mathbb{R}^m \times \mathbb{R}^n \rightarrow \mathbb{R}$  (for any  $j \in \{1, 2, \dots, J\}$ ) and the LL constraints  $h_{j'}(\mathbf{x}, \mathbf{y}) : \mathbb{R}^m \times \mathbb{R}^n \rightarrow \mathbb{R}$  (for any  $j' \in \{1, 2, \dots, J'\}$ ) are continuously differentiable functions. This is equivalent to  $\min_{\mathbf{x} \in \mathcal{X}} \varphi(\mathbf{x})$ , where  $\varphi(\mathbf{x})$ , the value-function of the sub-problem in Eq. (3), is adapted correspondingly to be

$$\varphi(\mathbf{x}) := \min_{\mathbf{y}} \left\{ F(\mathbf{x}, \mathbf{y}) : H_j(\mathbf{x}, \mathbf{y}) \leq 0, \forall j, \text{ and } \mathbf{y} \in \mathcal{S}(\mathbf{x}) \right\}.$$

Also, the counterpart for value-function of the LL problem is  $f^*(\mathbf{x}) := \min_{\mathbf{y}} \{f(\mathbf{x}, \mathbf{y}) : h_{j'}(\mathbf{x}, \mathbf{y}) \leq 0, \forall j'\}$ , and following the technique within Eq. (5) to transform the LL problem into an inequality constraint, the problem can be reformulated as

$$\begin{aligned} \varphi(\mathbf{x}) = \min_{\mathbf{y}} \left\{ F(\mathbf{x}, \mathbf{y}) : H_j(\mathbf{x}, \mathbf{y}) \leq 0, \forall j, \right. \\ \left. f(\mathbf{x}, \mathbf{y}) \leq f^*(\mathbf{x}), \text{ and } h_{j'}(\mathbf{x}, \mathbf{y}) \leq 0, \forall j' \right\}. \end{aligned} \quad (14)$$

After that, using the same idea of sequential minimization method, inspired by the regularized smoothing method in [46], the value-function  $f^*(\mathbf{x})$  can be approximated with a barrier function (different from Eq. (6) due to the LL constraints) and a regularization term:

$$f_{\mu, \sigma_B}^*(\mathbf{x}) = \min_{\mathbf{y}} \left\{ f(\mathbf{x}, \mathbf{y}) + \sum_{j'=1}^{J'} P_{B, \sigma_B}(h_{j'}(\mathbf{x}, \mathbf{y})) + \frac{\mu}{2} \|\mathbf{y}\|^2 \right\},$$

where  $P_{B, \sigma_B}(\omega) : \mathbb{R} \rightarrow \bar{\mathbb{R}}$  is the selected standard barrier function for the LL constraint  $h_{j'}$ , with  $\sigma_B$  as the barrier parameter. Note that here we define  $P_{B, \sigma_B}$  as a standard barrier function but not a modified barrier function. As for the approximation of  $\varphi(\mathbf{x})$ , Eq. (7) is transferred into

$$\begin{aligned} \varphi_{\mu, \theta, \sigma}(\mathbf{x}) = \min_{\mathbf{y}} \left\{ F(\mathbf{x}, \mathbf{y}) + \sum_{j=1}^J P_{H, \sigma_H}(H_j(\mathbf{x}, \mathbf{y})) \right. \\ \left. + \sum_{j'=1}^{J'} P_{h, \sigma_h}(h_{j'}(\mathbf{x}, \mathbf{y})) + P_{f, \sigma_f}(f(\mathbf{x}, \mathbf{y}) - f_{\mu, \sigma_B}^*(\mathbf{x})) + \frac{\theta}{2} \|\mathbf{y}\|^2 \right\}, \end{aligned}$$

where  $P_{H, \sigma_H}, P_{h, \sigma_h}, P_{f, \sigma_f} : \mathbb{R} \rightarrow \bar{\mathbb{R}}$  are the selected auxiliary functions of penalty or modified barrier with parameters  $\sigma_H, \sigma_h$  and  $\sigma_f$ , and  $(\mu, \theta, \sigma) = (\mu, \theta, \sigma_B, \sigma_H, \sigma_h, \sigma_f) > 0$ .

Then corresponding to Eq. (10) and Eq. (11), by denoting

$$\mathbf{z}_{\mu, \sigma_B}^*(\mathbf{x}) = \operatorname{argmin}_{\mathbf{y}} \left\{ f(\mathbf{x}, \mathbf{y}) + \sum_{j'=1}^{J'} P_{B, \sigma_B}(h_{j'}(\mathbf{x}, \mathbf{y})) + \frac{\mu}{2} \|\mathbf{y}\|^2 \right\},$$

and

$$\begin{aligned} \mathbf{y}_{\mu, \theta, \sigma}^*(\mathbf{x}) = \operatorname{argmin}_{\mathbf{y}} \left\{ F(\mathbf{x}, \mathbf{y}) + \sum_{j=1}^J P_{H, \sigma_H}(H_j(\mathbf{x}, \mathbf{y})) \right. \\ \left. + \sum_{j'=1}^{J'} P_{h, \sigma_h}(h_{j'}(\mathbf{x}, \mathbf{y})) + P_{f, \sigma_f}(f(\mathbf{x}, \mathbf{y}) - f_{\mu, \sigma_B}^*(\mathbf{x})) + \frac{\theta}{2} \|\mathbf{y}\|^2 \right\}, \end{aligned}$$

we have the next proposition, which follows the same idea to Proposition 1.

**Proposition 2** Suppose  $F(\mathbf{x}, \mathbf{y})$  and  $f(\mathbf{x}, \mathbf{y})$  are bounded below and continuously differentiable. Given  $\mathbf{x} \in \mathcal{X}$  and  $\mu, \theta, \sigma > 0$ , when  $\mathbf{z}_{\mu, \sigma_B}^*(\mathbf{x})$  and  $\mathbf{y}_{\mu, \theta, \sigma}^*(\mathbf{x})$  are unique, then  $\varphi_{\mu, \theta, \sigma}(\mathbf{x})$  is differentiable and

$$\begin{aligned} G(\mathbf{x}) = \left[ \sum_{j=1}^J \frac{\partial P_{H, \sigma_H}(H_j(\mathbf{x}, \mathbf{y}))}{\partial \mathbf{x}} + \sum_{j'=1}^{J'} \frac{\partial P_{h, \sigma_h}(h_{j'}(\mathbf{x}, \mathbf{y}))}{\partial \mathbf{x}} \right. \\ \left. + \frac{\partial P_{f, \sigma_f}(f(\mathbf{x}, \mathbf{y}) - f_{\mu, \sigma_B}^*(\mathbf{x}))}{\partial \mathbf{x}} \right] \Big|_{\mathbf{y}=\mathbf{y}_{\mu, \theta, \sigma}^*(\mathbf{x})}, \end{aligned}$$

where

$$\begin{aligned} f_{\mu, \sigma_B}^*(\mathbf{x}) = f(\mathbf{x}, \mathbf{z}_{\mu, \sigma_B}^*(\mathbf{x})) + \sum_{j'=1}^{J'} \frac{\partial P_{B, \sigma_B}(h_{j'}(\mathbf{x}, \mathbf{z}_{\mu, \sigma_B}^*(\mathbf{x})))}{\partial \mathbf{x}} \\ + \frac{\mu}{2} \|\mathbf{z}_{\mu, \sigma_B}^*(\mathbf{x})\|^2, \end{aligned}$$

and

$$\frac{\partial f_{\mu, \sigma_B}^*(\mathbf{x})}{\partial \mathbf{x}} = \left[ \frac{\partial f(\mathbf{x}, \mathbf{y})}{\partial \mathbf{x}} + \sum_{j'=1}^{J'} \frac{\partial P_{B, \sigma_B}(h_{j'}(\mathbf{x}, \mathbf{y}))}{\partial \mathbf{x}} \right] \Big|_{\mathbf{y}=\mathbf{z}_{\mu, \sigma_B}^*(\mathbf{x})}.$$

The proof is similar to Proposition 1, obtained by applying [45, Theorem 4.13, Remark 4.14]. The algorithm is then based on Proposition 2 and similar to Algorithm 1 and 2.

Note that in Section 4.1, our convergence analysis is carried out under this constrained setting, because problems without constraints can be regarded as a special case of it.

### 3.4 Extension for Pessimistic BLO

In this part, we consider the pessimistic BLO, which has been rarely discussed for handling learning tasks to our best knowledge. For brevity, we continue to consider problems without constraints on UL and LL, and this can be extended to the case with constraints easily. As what we have discussed about pessimistic BLO at the very beginning, its form is

$$\min_{\mathbf{x} \in \mathcal{X}} \max_{\mathbf{y} \in \mathbb{R}^n} F(\mathbf{x}, \mathbf{y}), \text{ s.t. } \mathbf{y} \in \mathcal{S}(\mathbf{x}) = \operatorname{argmin}_{\mathbf{y}} f(\mathbf{x}, \mathbf{y}). \quad (15)$$

Similar to the optimistic case, this problem can be transformed into  $\min_{\mathbf{x}} \varphi^p(\mathbf{x})$ , where the value-function  $\varphi(\mathbf{x})$  in Eq. (3) is redefined as

$$\varphi^p(\mathbf{x}) := \max_{\mathbf{y}} \left\{ F(\mathbf{x}, \mathbf{y}) : \mathbf{y} \in \mathcal{S}(\mathbf{x}) \right\}.$$

Then for the value-function  $f^*(\mathbf{x})$ , we have the same regularized  $f_{\mu}^*(\mathbf{x})$  to the optimistic case in Eq. (6). As for the approximation of  $\varphi^p(\mathbf{x})$ , thanks to the value-function-based sequential minimization, different from Eq. (7), we have

$$\varphi_{\mu, \theta, \sigma}^p(\mathbf{x}) = \max_{\mathbf{y}} \left\{ F(\mathbf{x}, \mathbf{y}) - P_{\sigma}(f(\mathbf{x}, \mathbf{y}) - f_{\mu}^*(\mathbf{x})) - \frac{\theta}{2} \|\mathbf{y}\|^2 \right\},$$

and same as before, our goal is to  $\min_{\mathbf{x}} \varphi_{\mu, \theta, \sigma}^p(\mathbf{x})$ .

Denote  $\mathbf{z}_{\mu}^*(\mathbf{x})$  to be the same as in Eq. (10), and Eq. (11) is changed into

$$\mathbf{y}_{\mu, \theta, \sigma}^*(\mathbf{x}) = \operatorname{argmax}_{\mathbf{y}} \left\{ F(\mathbf{x}, \mathbf{y}) - P_{\sigma}(f(\mathbf{x}, \mathbf{y}) - f_{\mu}^*(\mathbf{x})) - \frac{\theta}{2} \|\mathbf{y}\|^2 \right\}.$$

Then Proposition 1 in the optimistic case is changed into the following in the pessimistic case.

**Proposition 3** Suppose  $-F(\mathbf{x}, \mathbf{y})$  and  $f(\mathbf{x}, \mathbf{y})$  are bounded below and continuously differentiable. Given  $\mathbf{x} \in \mathcal{X}$  and  $\mu, \theta, \sigma > 0$ , when  $\mathbf{z}_{\mu}^*(\mathbf{x})$  and  $\mathbf{y}_{\mu, \theta, \sigma}^*(\mathbf{x})$  are unique, then  $\varphi_{\mu, \theta, \sigma}^p(\mathbf{x})$  is differentiable and

$$\frac{\partial \varphi_{\mu, \theta, \sigma}^p(\mathbf{x})}{\partial \mathbf{x}} = \frac{\partial F(\mathbf{x}, \mathbf{y}_{\mu, \theta, \sigma}^*(\mathbf{x}))}{\partial \mathbf{x}} + G(\mathbf{x}),$$

with

$$G(\mathbf{x}) = \frac{-\partial P_{\sigma}(f(\mathbf{x}, \mathbf{y}) - f_{\mu}^*(\mathbf{x}))}{\partial \mathbf{x}} \Big|_{\mathbf{y}=\mathbf{y}_{\mu, \theta, \sigma}^*(\mathbf{x})},$$

where  $f_\mu^*(\mathbf{x}) = f(\mathbf{x}, \mathbf{z}_\mu^*(\mathbf{x})) + \frac{\mu}{2} \|\mathbf{z}_\mu^*(\mathbf{x})\|^2$ , and  $\frac{\partial f_\mu^*(\mathbf{x})}{\partial \mathbf{x}} = \left. \frac{\partial f(\mathbf{x}, \mathbf{y})}{\partial \mathbf{x}} \right|_{\mathbf{y}=\mathbf{z}_\mu^*(\mathbf{x})}$ .

The proof is similar to Proposition 1, obtained by applying [45, Theorem 4.13, Remark 4.14]. The algorithm in the pessimistic case can then be derived similar to the optimistic case, but when calculating  $\mathbf{y}_{\mu, \theta, \sigma}^*(\mathbf{x})$ , gradient ascent is performed instead of gradient descent. In addition, the convergence of BVFSM for pessimistic BLO will be discussed in detail in Section 4.1.

## 4 THEORETICAL ANALYSIS

This section brings out the convergence analysis and complexity analysis of the proposed BVFSM.

### 4.1 Convergence Analysis

Here we show the convergence analysis of the proposed method. As BLO without constraints can be seen as a special case of BLO with constraints, regarding constraints as  $H_j(\mathbf{x}, \mathbf{y}) \equiv 0, \forall j$  and  $h_{j'}(\mathbf{x}, \mathbf{y}) \equiv 0, \forall j'$ , we prove the more general constrained case. Also, for brevity, we first prove in the optimistic BLO case, and the pessimistic case will be analyzed later in Corollary 1.

Note that for sequential-minimization-type scheme, including EGBMs and our BVFSM, people mainly focus on the approximation quality of these methods. That is, whether the solutions to sequential approximated sub-problems will converge to the solution to the original bi-level problem. Here we prove this kind of convergence from the aspect of global solution. We first recall an equivalent definition of epiconvergence given in [45, pp. 41].

**Definition 2**  $\varphi_k \xrightarrow{e} \varphi$  iff for all  $\mathbf{x} \in \mathbb{R}^m$ , the following two conditions hold:

- (1) for any sequence  $\{\mathbf{x}_k\}$  converging to  $\mathbf{x}$ ,

$$\liminf_{k \rightarrow \infty} \varphi_k(\mathbf{x}_k) \geq \varphi(\mathbf{x}); \quad (16)$$

- (2) there is a sequence  $\{\mathbf{x}_k\}$  converging to  $\mathbf{x}$  such that

$$\limsup_{k \rightarrow \infty} \varphi_k(\mathbf{x}_k) \leq \varphi(\mathbf{x}). \quad (17)$$

The convergence results are then given under the following statements as our blanket assumption for the problem:

#### Assumption 1 (Assumptions for the problem)

- (1)  $\mathcal{S}(\mathbf{x})$  is nonempty for  $\mathbf{x} \in \mathcal{X}$ .
- (2) Both  $F(\mathbf{x}, \mathbf{y})$  and  $f(\mathbf{x}, \mathbf{y})$  are jointly continuous and continuously differentiable. Both  $H_j(\mathbf{x}, \mathbf{y}), \forall j$  and  $h_{j'}(\mathbf{x}, \mathbf{y}), \forall j'$  are continuously differentiable.
- (3)  $F(\mathbf{x}, \mathbf{y})$  is level-bounded in  $\mathbf{y}$  locally uniformly in  $\mathbf{x} \in \mathcal{X}$  (see [29, Definition 3]).
- (4) 0 is not a local optimal value of  $h_{j'}(\mathbf{x}, \mathbf{y})$  with respect to  $\mathbf{y}$  for all  $j'$ .

For the simplicity of symbols, here we let  $j = j' = 1$ , meaning there is one constraint on the UL and LL problem respectively, and denote them as  $H(\mathbf{x}, \mathbf{y})$  and  $h(\mathbf{x}, \mathbf{y})$ . When  $j \neq 1$  or  $j' \neq 1$ , the proofs parallel actually. In addition, denote  $f_k^*(\mathbf{x}) := f_{\mu_k, \sigma_k}^*(\mathbf{x}), \varphi_k(\mathbf{x}) :=$

$\varphi_{\mu_k, \theta_k, \sigma_k}(\mathbf{x})$ , and  $P_k(\omega) := P_{\sigma_k}(\omega)$  defined in Eq. (8). Also,  $P_{B,k}(\omega), P_{H,k}(\omega), P_{h,k}(\omega), P_{f,k}(\omega)$  are defined similarly. Note that  $P_{B,k}$  is the standard barrier function, while  $P_{H,k}, P_{h,k}, P_{f,k}$  are the penalty or modified barrier functions. Then

$$f_k^*(\mathbf{x}) = \min_{\mathbf{y}} \left\{ f(\mathbf{x}, \mathbf{y}) + P_{B,k}(h(\mathbf{x}, \mathbf{y})) + \frac{\mu_k}{2} \|\mathbf{y}\|^2 \right\},$$

$$\begin{aligned} \varphi_k(\mathbf{x}) = \min_{\mathbf{y}} \left\{ F(\mathbf{x}, \mathbf{y}) + P_{H,k}(H(\mathbf{x}, \mathbf{y})) + P_{h,k}(h(\mathbf{x}, \mathbf{y})) \right. \\ \left. + P_{f,k}(f(\mathbf{x}, \mathbf{y}) - f_k^*(\mathbf{x})) + \frac{\theta_k}{2} \|\mathbf{y}\|^2 \right\}. \end{aligned}$$

To begin with, we present the following lemma on the properties of penalty and modified barrier functions, as the preparation for further discussion and proofs.

**Lemma 1** Let  $\{(\mu_k, \theta_k, \sigma_k)\}$  be a positive sequence such that  $\lim_{k \rightarrow \infty} (\mu_k, \theta_k, \sigma_k) = 0$ . Additionally assume that  $\lim_{k \rightarrow \infty} \rho(-\sigma_k^{(2)}; \sigma_k^{(1)}) = 0$  when  $\rho$  is a modified barrier function. Then we have

- (1)  $P_k(\omega)$  is continuous, differentiable and non-decreasing, and satisfies  $P_k(\omega) \geq 0$ .
- (2) For any  $\omega \leq 0$ ,  $\lim_{k \rightarrow \infty} P_k(\omega) = 0$ .
- (3) For any sequence  $\{\omega_k\}$ ,  $\lim_{k \rightarrow \infty} P_k(\omega_k) < +\infty$  implies that  $\limsup_{k \rightarrow \infty} \omega_k \leq 0$ .

*Proof:* From the definitions of standard penalty and barrier functions (see, e.g., Definition 1), the statement (1) follows immediately.

When  $\rho$  is a penalty function,  $\lim_{\sigma \rightarrow 0} \rho(\omega; \sigma)$  is equal to  $+\infty$  for  $\omega > 0$  and 0 for  $\omega \leq 0$ . Hence, as  $k \rightarrow \infty, \sigma_k \rightarrow 0$ , we have  $P_k(\omega) \rightarrow 0$ , for  $\omega \leq 0$ . For any sequence  $\{\omega_k\}$ , if  $\limsup_{k \rightarrow \infty} \omega_k > 0$ , there exist a subsequence  $\{\omega_t\}$  of  $\{\omega_k\}$  and  $\varepsilon > 0$  such that  $\omega_t \geq \varepsilon$  for all  $t$ . Then, it follows from the monotonicity of  $\rho$  that  $\lim_{t \rightarrow \infty} P_t(\omega_t) = \lim_{t \rightarrow \infty} \rho(\omega_t; \sigma_t) \geq \lim_{t \rightarrow \infty} \rho(\varepsilon; \sigma_t) = +\infty$ . Thus,  $\lim_{k \rightarrow \infty} P_k(\omega_k) < +\infty$  implies that  $\limsup_{k \rightarrow \infty} \omega_k \leq 0$ .

If  $\rho$  is a modified barrier function, since  $\rho$  is non-decreasing, we have  $0 \leq \rho(\omega - \sigma_k^{(2)}; \sigma_k^{(1)}) \leq \rho(-\sigma_k^{(2)}; \sigma_k^{(1)})$  when  $\omega \leq 0$ . The assumption  $\lim_{k \rightarrow \infty} \rho(-\sigma_k^{(2)}; \sigma_k^{(1)}) = 0$  implies  $\rho(\omega - \sigma_k^{(2)}; \sigma_k^{(1)}) \rightarrow 0$  when  $\omega \leq 0$ . Hence, as  $k \rightarrow \infty$ , we have  $\sigma_k^{(1)} \rightarrow 0, \sigma_k^{(2)} \rightarrow 0$ , and  $P_k(\omega) \rightarrow 0$ , for  $\omega \leq 0$ . For any sequence  $\{\omega_k\}$ , if  $\lim_{k \rightarrow \infty} P_k(\omega_k) < +\infty$ , then it follows from the definition of modified barrier function that  $\omega_k \leq \sigma_k^{(2)}$  and (3) follows immediately from  $\sigma_k^{(2)} \rightarrow 0$ .  $\square$

We will use these properties in later proofs, so we hold these requirements on parameters in Lemma 1 from now on.

To prove the convergence result, we show that  $\varphi_k(\mathbf{x}) + \delta_{\mathcal{X}}(\mathbf{x}) \xrightarrow{e} \varphi(\mathbf{x}) + \delta_{\mathcal{X}}(\mathbf{x})$ , where  $\delta_{\mathcal{X}}(\mathbf{x})$  denotes the indicator function of the set  $\mathcal{X}$ , i.e.,  $\delta_{\mathcal{X}}(\mathbf{x}) = 0$  if  $\mathbf{x} \in \mathcal{X}$  and  $\delta_{\mathcal{X}}(\mathbf{x}) = +\infty$  if  $\mathbf{x} \notin \mathcal{X}$ . Hence, we need to verify two conditions given in Definition 2.

First, to prove the first condition Eq. (16) in Definition 2, we propose the following two lemmas.

**Lemma 2** Let  $\{(\mu_k, \sigma_k)\}$  be a positive sequence such that  $(\mu_k, \sigma_k) \rightarrow 0$ , satisfying the same setting as in Lemma 1. Then for any sequence  $\{\mathbf{x}_k\}$  converging to  $\bar{\mathbf{x}}$ ,

$$\limsup_{k \rightarrow \infty} f_k^*(\mathbf{x}_k) \leq f^*(\bar{\mathbf{x}}).$$

*Proof:* Given any  $\epsilon > 0$ , there exists  $\bar{\mathbf{y}} \in \mathbb{R}^m$  such that  $f(\bar{\mathbf{x}}, \bar{\mathbf{y}}) < f^*(\bar{\mathbf{x}}) + 1/2 \epsilon$ , and  $h(\bar{\mathbf{x}}, \bar{\mathbf{y}}) \leq 0$ . If  $h(\bar{\mathbf{x}}, \bar{\mathbf{y}}) = 0$ , by Assumption 1.(4), the minimum of  $h$  with respect to  $\mathbf{y}$  in any neighbourhood of  $\bar{\mathbf{y}}$  is smaller than 0, so we can find a  $\hat{\mathbf{y}}$  close enough to  $\bar{\mathbf{y}}$  such that  $f(\bar{\mathbf{x}}, \hat{\mathbf{y}}) < f^*(\bar{\mathbf{x}}) + \epsilon$ , and  $h(\bar{\mathbf{x}}, \hat{\mathbf{y}}) \leq -\delta$  for some  $\delta > 0$ . If  $h(\bar{\mathbf{x}}, \bar{\mathbf{y}}) < 0$ , such  $\hat{\mathbf{y}}$  exists obviously.

As  $\{\mathbf{x}_k\}$  converges to  $\bar{\mathbf{x}}$ ,  $h(\bar{\mathbf{x}}, \hat{\mathbf{y}}) \leq -\delta$  combining with the continuity of  $h(\mathbf{x}, \mathbf{y})$  implies the existence of  $K_1 > 0$  such that  $h(\mathbf{x}_k, \hat{\mathbf{y}}) \leq -\delta/2$  for all  $k \geq K_1$ . Since the barrier function is non-decreasing, it follows that  $P_{B,k}(h(\mathbf{x}_k, \hat{\mathbf{y}})) \leq \rho(-\delta/2; \sigma_k^{(1)})$ . Then  $\lim_{k \rightarrow \infty} \rho(-\delta/2; \sigma_k^{(1)}) = 0$  yields

$$\lim_{k \rightarrow \infty} P_{B,k}(h(\mathbf{x}_k, \hat{\mathbf{y}})) = 0.$$

Next, as  $\{\mathbf{x}_k\}$  converges to  $\bar{\mathbf{x}}$ , it follows from the continuity of  $f(\mathbf{x}, \mathbf{y})$  and  $\mu_k \rightarrow 0$  that there exists  $K_2 \geq K_1$ , such that for any  $k \geq K_2$ ,

$$\begin{aligned} f_k^*(\mathbf{x}_k) &\leq f(\mathbf{x}_k, \hat{\mathbf{y}}) + P_{B,k}(h(\mathbf{x}_k, \hat{\mathbf{y}})) + \frac{\mu_k}{2} \|\hat{\mathbf{y}}\|^2 \\ &\leq f(\bar{\mathbf{x}}, \hat{\mathbf{y}}) + \epsilon \\ &\leq f^*(\bar{\mathbf{x}}) + 2\epsilon. \end{aligned}$$

By letting  $k \rightarrow \infty$ , we obtain

$$\limsup_{k \rightarrow \infty} f_k^*(\mathbf{x}_k) \leq f^*(\bar{\mathbf{x}}) + 2\epsilon,$$

and taking  $\epsilon \rightarrow 0$  in the above inequality yields the conclusion.  $\square$

**Lemma 3** Given  $\bar{\mathbf{x}} \in \mathcal{X}$ , let  $\{(\mu_k, \theta_k, \sigma_k)\}$  satisfies the same setting as in Lemma 1, and then for any sequence  $\{\mathbf{x}_k\}$  converging to  $\bar{\mathbf{x}}$ ,

$$\liminf_{k \rightarrow \infty} \varphi_k(\mathbf{x}_k) \geq \varphi(\bar{\mathbf{x}}).$$

*Proof:* We assume by contradiction that there exists  $\bar{\mathbf{x}} \in \mathcal{X}$  and a sequence  $\{\mathbf{x}_k\}$ , satisfying  $\mathbf{x}_k \rightarrow \bar{\mathbf{x}}$  as  $k \rightarrow \infty$  with the following inequality

$$\lim_{k \rightarrow \infty} \varphi_k(\mathbf{x}_k) < \varphi(\bar{\mathbf{x}}).$$

Then, there exist  $\epsilon > 0$  and a sequence  $\{\mathbf{y}_k\}$  satisfying

$$\begin{aligned} F(\mathbf{x}_k, \mathbf{y}_k) + P_{H,k}(H(\mathbf{x}_k, \mathbf{y}_k)) + P_{h,k}(h(\mathbf{x}_k, \mathbf{y}_k)) \\ + P_{f,k}(f(\mathbf{x}_k, \mathbf{y}_k) - f_k^*(\mathbf{x}_k)) + \frac{\theta_k}{2} \|\mathbf{y}_k\|^2 < \varphi(\bar{\mathbf{x}}) - \epsilon. \end{aligned} \quad (18)$$

Since  $F(\mathbf{x}, \mathbf{y})$  is level-bounded in  $\mathbf{y}$  locally uniformly in  $\bar{\mathbf{x}}$ , we have that  $\{\mathbf{y}_k\}$  is bounded. Take a subsequence  $\{\mathbf{y}_t\}$  of  $\{\mathbf{y}_k\}$  which satisfies there exists  $\hat{\mathbf{y}}$ , such that  $\mathbf{y}_t \rightarrow \hat{\mathbf{y}}$ .

The inequality Eq. (18) yields that

$$P_{f,t}(f(\mathbf{x}_t, \mathbf{y}_t) - f_t^*(\mathbf{x}_t)) < \varphi(\bar{\mathbf{x}}) - \epsilon - F(\mathbf{x}_t, \mathbf{y}_t).$$

Taking  $t \rightarrow \infty$  then  $\lim_{t \rightarrow \infty} P_{f,t}(f(\mathbf{x}_t, \mathbf{y}_t) - f_t^*(\mathbf{x}_t)) < +\infty$ . From Lemma 1, we have  $\limsup_{t \rightarrow \infty} \{f(\mathbf{x}_t, \mathbf{y}_t) - f_t^*(\mathbf{x}_t)\} \leq 0$ , and hence by the continuity of  $f$ ,

$$\lim_{t \rightarrow \infty} f(\mathbf{x}_t, \mathbf{y}_t) \leq \liminf_{t \rightarrow \infty} f_t^*(\mathbf{x}_t).$$

Then, by the continuity of  $f$  and Lemma 2, we have

$$f(\bar{\mathbf{x}}, \hat{\mathbf{y}}) = \lim_{t \rightarrow \infty} f(\mathbf{x}_t, \mathbf{y}_t) \leq \limsup_{t \rightarrow \infty} f_t^*(\mathbf{x}_t) \leq f^*(\bar{\mathbf{x}}).$$

By using similar arguments and the continuity of  $h$  and  $H$ , one can show  $h(\bar{\mathbf{x}}, \hat{\mathbf{y}}) \leq 0$  and  $H(\bar{\mathbf{x}}, \hat{\mathbf{y}}) \leq 0$ . Thus, we have  $\hat{\mathbf{y}} \in S(\bar{\mathbf{x}})$ , and  $\hat{\mathbf{y}}$  is a feasible point to problem Eq. (14) with  $\mathbf{x} = \bar{\mathbf{x}}$ . Then Eq. (18) yields

$$\varphi(\bar{\mathbf{x}}) \leq F(\bar{\mathbf{x}}, \hat{\mathbf{y}}) \leq \limsup_{k \rightarrow \infty} F(\mathbf{x}_k, \mathbf{y}_k) \leq \varphi(\bar{\mathbf{x}}) - \epsilon,$$

which implies a contradiction. Thus we get the conclusion.  $\square$

Next, we verify the second condition Eq. (17) in Definition 2.

**Lemma 4** Let  $\{(\mu_k, \theta_k, \sigma_k)\}$  satisfies the same setting as in Lemma 1, then for any  $\mathbf{x} \in \mathcal{X}$ ,

$$\limsup_{k \rightarrow \infty} \varphi_k(\mathbf{x}) \leq \varphi(\mathbf{x}).$$

*Proof:* Given any  $\bar{\mathbf{x}} \in \mathcal{X}$ , for any  $\epsilon > 0$ , there exists  $\bar{\mathbf{y}} \in \mathbb{R}^m$  satisfying  $f(\bar{\mathbf{x}}, \bar{\mathbf{y}}) \leq f^*(\bar{\mathbf{x}})$ ,  $h(\bar{\mathbf{x}}, \bar{\mathbf{y}}) \leq 0$ ,  $H(\bar{\mathbf{x}}, \bar{\mathbf{y}}) \leq 0$ , and  $F(\bar{\mathbf{x}}, \bar{\mathbf{y}}) \leq \varphi(\bar{\mathbf{x}}) + \epsilon$ .

By the definition of  $\varphi_k$ , we have

$$\begin{aligned} \varphi_k(\bar{\mathbf{x}}) &\leq F(\bar{\mathbf{x}}, \bar{\mathbf{y}}) + P_{H,k}(H(\bar{\mathbf{x}}, \bar{\mathbf{y}})) + P_{h,k}(h(\bar{\mathbf{x}}, \bar{\mathbf{y}})) \\ &\quad + P_{f,k}(f(\bar{\mathbf{x}}, \bar{\mathbf{y}}) - f_k^*(\bar{\mathbf{x}})) + \frac{\theta_k}{2} \|\bar{\mathbf{y}}\|^2. \end{aligned} \quad (19)$$

From Lemma 1, as  $k \rightarrow \infty$ , we have  $P_{H,k}(H(\bar{\mathbf{x}}, \bar{\mathbf{y}})) \rightarrow 0$ , and  $P_{h,k}(h(\bar{\mathbf{x}}, \bar{\mathbf{y}})) \rightarrow 0$ . As we choose the standard barrier function for  $P_{B,k}$  in the definition of  $f_k^*(\mathbf{x})$ , thus  $f(\mathbf{x}, \mathbf{y}) + P_{B,k}(h(\mathbf{x}, \mathbf{y})) + \frac{\mu_k}{2} \|\mathbf{y}\|^2$  is always larger than  $f(\mathbf{x}, \mathbf{y})$  for any  $\mathbf{x}$  and  $\mathbf{y}$  feasible to the LL problem, and hence  $f_k^*(\bar{\mathbf{x}}) \geq f^*(\bar{\mathbf{x}})$ . Then we have  $f(\bar{\mathbf{x}}, \bar{\mathbf{y}}) - f_k^*(\bar{\mathbf{x}}) \leq f(\bar{\mathbf{x}}, \bar{\mathbf{y}}) - f^*(\bar{\mathbf{x}}) \leq 0$ . Then it follows from the monotonicity of  $P_{f,k}$  and Lemma 1 that  $P_{f,k}(f(\bar{\mathbf{x}}, \bar{\mathbf{y}}) - f_k^*(\bar{\mathbf{x}})) \rightarrow 0$ .

Therefore, as  $\theta_k \rightarrow 0$ , by taking  $k \rightarrow \infty$  in inequality Eq. (19), we have

$$\limsup_{k \rightarrow \infty} \varphi_k(\bar{\mathbf{x}}) \leq \varphi(\bar{\mathbf{x}}) + \epsilon.$$

Then, we get the conclusion by letting  $\epsilon \rightarrow 0$ .  $\square$

Now, by combining the results obtained above, we can obtain the desired epiconvergence result, which also indicates the convergence of our method.

### Theorem 1 (Convergence for Optimistic BLO)

Let  $\{(\mu_k, \theta_k, \sigma_k)\}$  be a positive sequence such that  $(\mu_k, \theta_k, \sigma_k) \rightarrow 0$ , satisfying the same setting as in Lemma 1.

(1) The epiconvergence holds:

$$\varphi_k(\mathbf{x}) + \delta_{\mathcal{X}}(\mathbf{x}) \xrightarrow{e} \varphi(\mathbf{x}) + \delta_{\mathcal{X}}(\mathbf{x}).$$

(2) We have the following inequality:

$$\limsup_{k \rightarrow \infty} \left( \inf_{\mathbf{x} \in \mathcal{X}} \varphi_k(\mathbf{x}) \right) \leq \inf_{\mathbf{x} \in \mathcal{X}} \varphi(\mathbf{x}).$$

In addition, if  $\mathbf{x}_\ell \in \operatorname{argmin}_{\mathbf{x} \in \mathcal{X}} \varphi_\ell(\mathbf{x})$  for some subsequence  $\{\ell\} \subset \mathbb{N}$ , and  $\mathbf{x}_\ell$  converges to  $\tilde{\mathbf{x}}$ , then  $\tilde{\mathbf{x}} \in \operatorname{argmin}_{\mathbf{x} \in \mathcal{X}} \varphi(\mathbf{x})$  and

$$\lim_{\ell \rightarrow \infty} \left( \inf_{\mathbf{x} \in \mathcal{X}} \varphi_\ell(\mathbf{x}) \right) = \inf_{\mathbf{x} \in \mathcal{X}} \varphi(\mathbf{x}).$$

*Proof:* To prove the epiconvergence of  $\varphi_k$  to  $\varphi$ , we just need to verify that the sequence  $\{\varphi_k\}$  satisfies the two



TABLE 2

Comparison among existing methods and our BVFSM. We present the convergence results, conditions required for convergence, whether it needs the LLC condition, whether it can be extended to BLO with constraints and pessimistic BLO, respectively for each method.

Category	Method	Convergence Results	Required Conditions	LLC	Constraints	Pessimistic
EGBMs	FHG/RHG	$\mathbf{x}_k \xrightarrow{s} \mathbf{x}^*$ $\inf_{\mathbf{x} \in \mathcal{X}} \varphi_k(\mathbf{x}) \rightarrow \inf_{\mathbf{x} \in \mathcal{X}} \varphi(\mathbf{x})$	$F(\mathbf{x}, \mathbf{y})$ and $f(\mathbf{x}, \mathbf{y})$ are $C^1$ .	✓	✗	✗
	TRHG	$\mathbf{x}_k \rightarrow \hat{\mathbf{x}}^*$	$F(\mathbf{x}, \mathbf{y})$ is $C^1$ and bounded below; $f(\mathbf{x}, \mathbf{y})$ is $C^1$ , $L_f$ -smooth and strongly convex.	✓	✗	✗
	BDA	$\mathbf{x}_k \xrightarrow{s} \mathbf{x}^*$ $\inf_{\mathbf{x} \in \mathcal{X}} \varphi_k(\mathbf{x}) \rightarrow \inf_{\mathbf{x} \in \mathcal{X}} \varphi(\mathbf{x})$	$F(\mathbf{x}, \mathbf{y})$ is $L_F$ -smooth, convex, bounded below; $f(\mathbf{x}, \mathbf{y})$ is $L_f$ -smooth.	✓	✗	✗
IGBMs	CG/Neumann	$\mathbf{x}_k \rightarrow \hat{\mathbf{x}}^*$	$F(\mathbf{x}, \mathbf{y})$ and $f(\mathbf{x}, \mathbf{y})$ are $C^1$ ; $\frac{\partial^2 f(\mathbf{x}, \mathbf{y})}{\partial \mathbf{y} \partial \mathbf{y}}$ is invertible.	✓	✗	✗
Ours	BVFSM	$\mathbf{x}_k \xrightarrow{s} \mathbf{x}^*$ $\inf_{\mathbf{x} \in \mathcal{X}} \varphi_k(\mathbf{x}) \rightarrow \inf_{\mathbf{x} \in \mathcal{X}} \varphi(\mathbf{x})$	$F(\mathbf{x}, \mathbf{y})$ and $f(\mathbf{x}, \mathbf{y})$ are $C^1$ and level-bounded.	✗	✓	✓

<sup>1</sup>  $C^1$  denotes continuously differentiable.  $L_f$  (or  $L_F$ )-smooth means the gradient of  $f$  (or  $F$ ) is Lipschitz continuous with Lipschitz constant  $L_f$  (or  $L_F$ ). “Level-bounded” is short for “level-bounded in  $\mathbf{y}$  locally uniformly in  $\mathbf{x} \in \mathcal{X}$ ”.

<sup>2</sup> The arrow  $\xrightarrow{s}$  represents the subsequential convergence.  $\mathbf{x}^*$  denotes the optimal solution, and  $\hat{\mathbf{x}}^*$  denotes the stationary point.

TABLE 3

Comparison of computational complexity results among BVFSM and existing gradient-based methods. We show the key update ideas for calculating  $G(\mathbf{x})$  in  $\frac{\partial \varphi(\mathbf{x})}{\partial \mathbf{x}}$ . Please see [2], [27], [28] for more details of EGBMs and IGBMs. Note that our method avoids solving an unrolled dynamic system or approximating the inverse of Hessian.

Category	Method	Key point for calculating $G(\mathbf{x})$	Time	Space
EGBMs	FHG	Forward propagation with repeated matrix-matrix multiplication	$O(m^2 n T)$	$O(mn)$
	RHG	Backward propagation with repeated matrix-vector multiplication	$O(n(m+n)T)$	$O(m+nT)$
	TRHG	Similar to RHG, but truncate the trajectory	$O(n(m+n)I)$	$O(m+nI)$
	BDA	Similar to RHG, but combines UL and LL objectives	$O(n(m+n)T)$	$O(m+nT)$
IGBMs	CG	Approximating the inverse of Hessian by solving linear systems	$O(m+nT+n^2Q)$	$O(m+n)$
	Neumann	Approximating the inverse of Hessian by Neumann series	$O(m+nT+n^2Q)$	$O(m+n)$
Ours	BVFSM	A simple combination of the gradients of two regularized functions	$O(m+n(T_z+T_y))$	$O(m+n)$

conditions given in Definition 2. Considering any sequence  $\{\mathbf{x}_k\}$  converging to  $\mathbf{x}$ , if  $\mathbf{x} \in \mathcal{X}$ , we obtain from Lemma 3 that

$$\begin{aligned}
 \varphi(\mathbf{x}) + \delta_{\mathcal{X}}(\mathbf{x}) &= \varphi(\mathbf{x}) \\
 &\leq \liminf_{k \rightarrow \infty} \varphi_k(\mathbf{x}_k) \\
 &\leq \liminf_{k \rightarrow \infty} \varphi_k(\mathbf{x}_k) + \delta_{\mathcal{X}}(\mathbf{x}_k).
 \end{aligned}$$

When  $\mathbf{x} \notin \mathcal{X}$ , we have  $\liminf_{k \rightarrow \infty} \varphi_k(\mathbf{x}_k) + \delta_{\mathcal{X}}(\mathbf{x}_k) = +\infty$  because  $\mathcal{X}$  is closed. Thus the first condition Eq. (16) in Definition 2 is satisfied.

Next, for any  $\mathbf{x} \in \mathbb{R}^m$ , if  $\mathbf{x} \in \mathcal{X}$ , then it follows from Lemma 4 that

$$\begin{aligned}
 \limsup_{k \rightarrow \infty} \varphi_k(\mathbf{x}) + \delta_{\mathcal{X}}(\mathbf{x}) &= \limsup_{k \rightarrow \infty} \varphi_k(\mathbf{x}) \\
 &\leq \varphi(\mathbf{x}) = \varphi(\mathbf{x}) + \delta_{\mathcal{X}}(\mathbf{x}).
 \end{aligned}$$

When  $\mathbf{x} \notin \mathcal{X}$ , we have  $\varphi(\mathbf{x}) + \delta_{\mathcal{X}}(\mathbf{x}) = +\infty$ . Thus the second condition Eq. (17) in Definition 2 is satisfied. Therefore, we get the conclusion (1) immediately from Definition 2. Then

the conclusion (2) follows from [45, Proposition 4.6].  $\square$

Next, we consider the convergence for pessimistic BLO. To begin with, for pessimistic BLO without functional constraints, we denote  $\varphi_k^p(\mathbf{x})$  similarly to the optimistic case:

$$\begin{aligned}
 \varphi_k^p(\mathbf{x}) &:= \varphi_{\mu_k, \theta_k, \sigma_k}^p(\mathbf{x}) \\
 &= \max_{\mathbf{y}} \left\{ F(\mathbf{x}, \mathbf{y}) - P_k(f(\mathbf{x}, \mathbf{y}) - f_k^*(\mathbf{x})) - \frac{\theta_k}{2} \|\mathbf{y}\|^2 \right\},
 \end{aligned}$$

where  $f_k^*(\mathbf{x}) = \min_{\mathbf{y}} \{f(\mathbf{x}, \mathbf{y}) + \frac{\mu_k}{2} \|\mathbf{y}\|^2\}$ . Then we have the following corollary. Note that this convergence result can also be extended to pessimistic BLO with constraints easily.

#### Corollary 1 (Convergence for Pessimistic BLO)

Let  $\{(\mu_k, \theta_k, \sigma_k)\}$  be a positive sequence such that  $(\mu_k, \theta_k, \sigma_k) \rightarrow 0$ , satisfying the same setting as in Lemma 1. Then we have the following inequality:

$$\limsup_{k \rightarrow \infty} \left( \inf_{\mathbf{x} \in \mathcal{X}} \varphi_k^p(\mathbf{x}) \right) \leq \inf_{\mathbf{x} \in \mathcal{X}} \varphi^p(\mathbf{x}).$$

In addition, if  $\mathbf{x}_\ell \in \operatorname{argmin}_{\mathbf{x} \in \mathcal{X}} \varphi_\ell^p(\mathbf{x})$  for some subsequence  $\{\ell\} \subset \mathbb{N}$ , and  $\mathbf{x}_\ell$  converges to  $\tilde{\mathbf{x}}$ , then  $\tilde{\mathbf{x}} \in \operatorname{argmin}_{\mathbf{x} \in \mathcal{X}} \varphi^p(\mathbf{x})$  and

$$\lim_{\ell \rightarrow \infty} \left( \inf_{\mathbf{x} \in \mathcal{X}} \varphi_\ell^p(\mathbf{x}) \right) = \inf_{\mathbf{x} \in \mathcal{X}} \varphi^p(\mathbf{x}).$$

*Proof:* Based on the idea to prove Theorem 1, we first need to prove  $\varphi_k^p(\mathbf{x}) + \delta_{\mathcal{X}}(\mathbf{x}) \xrightarrow{e} \varphi^p(\mathbf{x}) + \delta_{\mathcal{X}}(\mathbf{x})$  by Lemma 1, 2, 3, and 4. Lemma 1 and 2 are unrelated to whether it is the optimistic or pessimistic case, and thus holds naturally. For Lemma 3 and 4, their corresponding results can be derived simply by replacing  $F$  in their proof with  $-F$ . Then the conclusion can be obtained with the same proof as in Theorem 1.  $\square$

In Table 2, we present the comparison among existing methods and our BVFSM, including the convergence results, conditions required for convergence, whether it needs the LLC condition, whether it can be extended to BLO with constraints and pessimistic BLO, respectively for each method. It can be seen that under mild assumptions, BVFSM is able to obtain convergence without LLC restrictive in real tasks, and be applied in problems with constraints and pessimistic BLO, which is not available by other methods.

## 4.2 Complexity Analysis

In this part, we compare the time and space complexity of Algorithms 2 with EGBMs (i.e., FHG, RHG, TRHG and BDA) and IGBMs (i.e., CG and Neumann) for computing  $G(\mathbf{x})$  or  $\frac{\partial \varphi(\mathbf{x})}{\partial \mathbf{x}}$ , i.e., the direction for updating variable  $\mathbf{x}$ . Table 3 summarizes the complexity results. Our complexity analysis follows the assumptions in [5]. For all existing methods, we assume solving the optimal solution of the LL problem, also the transition function  $\Phi$  in EGBMs for obtaining  $\mathbf{y}_T(\mathbf{x})$ , is the process of a  $T$ -step gradient descent.

**EGBMs.** As discussed in [2], [26], after implementing  $T$  steps of gradient descent with time complexity and space complexity of  $O(n)$  to solve the LL problem, FHG for forward calculation of Hessian-matrix product can be evaluated in time  $O(m^2 n T)$  and space  $O(mn)$ , and RHG for reverse calculation of Hessian- and Jacobian-vector products can be evaluated in time  $O(n(m+n)T)$  and space  $O(m+nT)$ . TRHG truncates the length of back-propagation trajectory to  $I$  after a  $T$ -step gradient descent, and thus reduces the time and space complexity to  $O(n(m+n)I)$  and space  $O(m+nI)$ . BDA uses the same idea to RHG, except that it combines UL and LL objectives during back propagation, so the order of complexity of time and space is the same to RHG. The time complexity for EGBMs to calculate the UL gradient is proportional to  $T$ , the number of iterations of the LL problem, and thus EGBMs take a large amount of time to ensure convergence.

**IGBMs.** After implementing a  $T$ -step gradient descent for the LL problem, IGBMs approximate the inverse of Hessian matrix by conjugate gradient (CG), which solves a linear system of  $Q$  steps, or by Neumann series. Note that each step of CG and Neumann method includes Hessian-vector products, requiring  $O(m+n^2Q)$  time and  $O(m+n)$  space, so IGBMs run in time  $O(m+nT+n^2Q)$  and space  $O(m+n)$ . IGBMs decouple the complexity of calculating the UL gradient from being proportional to  $T$ , but the iteration

number  $Q$  always relies on the properties of the Hessian matrix, and in some cases,  $Q$  can be much larger than  $T$ .

**BVFSM.** In our algorithm, it takes time  $O(nT_z)$  and space  $O(n)$  to calculate  $T_z$  steps of gradient descent on Eq. (10) for the solution of LL problem  $\mathbf{z}^{T_z}$ . Then  $T_y$  steps of gradient descent on Eq. (11) are used to calculate  $\mathbf{y}^{T_y}$ , which requires time  $O(nT_y)$  and space  $O(n)$ . After that, the direction can be obtained according to the formula given in Eq. (13) by several computations of the gradient  $\frac{\partial f}{\partial \mathbf{x}}$  and  $\frac{\partial F}{\partial \mathbf{x}}$  without any intermediate update, which requires time  $O(m)$  and space  $O(m+n)$ . Therefore, BVFSM runs in time  $O(m+n(T_z+T_y))$  and space  $O(m+n)$  each time, respectively.

It can be observed from Table 3 that BVFSM needs less space than EGBMs, and as for time complexity, our method takes much less time than EGBMs and IGBMs, especially when  $n$  is large, meaning the LL problem is high-dimensional, for example, in applications with a large-scale network. Overall, this is because BVFSM does not need any computation of Hessian- or Jacobian-vector products for solving the unrolled dynamic system by recurrent iteration or approximating the inverse of Hessian, and all of the complexity comes from calculating the gradients of  $F$  and  $f$ , but calculating gradient is much easier than calculating Hessian- and Jacobian-vector products (even by AD). Besides, although BVFSM has the same order of space complexity to IGBMs, it is indeed smaller, because the memory is saved by eliminating the need to save the computational graph used for calculating Hessian. We will further illustrate these advantages through numerical results in Section 5.

## 5 EXPERIMENTAL RESULTS

In this section, we quantitatively demonstrate the performance of our BVFSM, especially when dealing with complicated and high-dimensional problems, and start with investigating the convergence accuracy and computational burden of the proposed optimization algorithm on numerical examples in Section 5.1. Then in Section 5.2, we apply BVFSM in the hyper-parameter optimization for hyper-cleaning on the widely-used MNIST, FashionMNIST and CIFAR-10 datasets under different settings to further study the impact of network structure and types of auxiliary functions. To further validate the generality of our method, we conduct experiments on other tasks such as few-shot learning in Section 5.3 and GAN in Section 5.4. The experiments were done on a PC with Intel Core i7-9700K CPU (4.2 GHz), 32GB RAM and an NVIDIA GeForce RTX 2060S GPU with 8GB VRAM, and the algorithm was implemented using PyTorch 1.6. We use the implementation in [47], [38] for the existing methods. We use MB (MegaByte) and S (Second) as the evaluation units of space and time complexity, respectively.

### 5.1 Numerical Evaluations

We use a numerical example with a non-convex LL which can adjust various dimensions to validate our effectiveness of BVFSM over existing methods. In particular, we use the following numerical example:

$$\begin{aligned} \min_{\mathbf{x} \in \mathbb{R}, \mathbf{y} \in \mathbb{R}^n} \quad & \|\mathbf{x} - a\|^2 + \|\mathbf{y} - a - \mathbf{c}\|^2 \\ \text{s.t. } \quad & [\mathbf{y}]_i \in \operatorname{argmin}_{[\mathbf{y}]_i \in \mathbb{R}} \sin(\mathbf{x} + [\mathbf{y}]_i - [\mathbf{c}]_i), \forall i, \end{aligned} \quad (20)$$

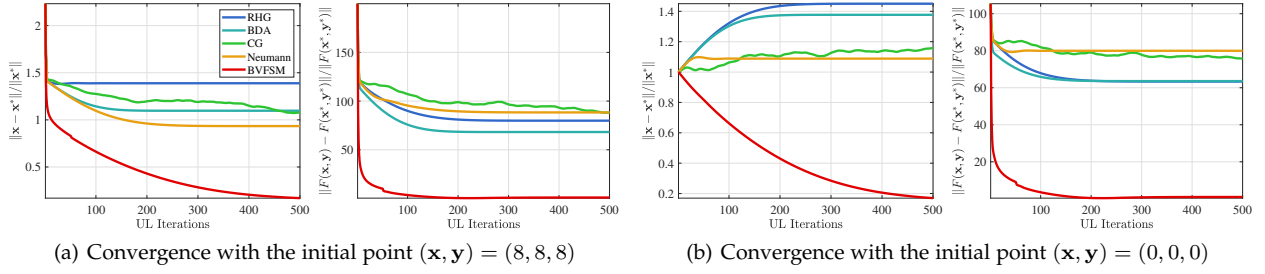


Fig. 1. The convergence behavior of various gradient-based BLO algorithms under different initial points. The (1st,3rd) and (2nd,4th) subfigures respectively show the errors of UL variable (i.e.,  $\|x - x^*\|/\|x^*\|$ ) and UL objective (i.e.,  $\|F(x, y) - F(x^*, y^*)\|/\|F(x^*, y^*)\|$ ). The legend is only plotted in the first subfigure.

where  $[y]_i$  denotes the  $i$ -th component of  $y$ , while  $a \in \mathbb{R}$  and  $c \in \mathbb{R}^n$  are adjustable parameters set as  $a = 2$  and  $[c]_i = 2$ , for any  $i = 1, 2, \dots, n$ . Note that here in the numerical example,  $x \in \mathbb{R}$  is a one-dimensional real number, and we still use the bold letter to represent the scalar in order to maintain the consistency of the context. The solution of such problem is

$$x = \frac{(1-n)a + nC}{1+n}, \text{ and } [y]_i = C + [c]_i - x, \forall i,$$

where

$$C = \operatorname{argmin}_C \left\{ \|C - 2a\| : C = -\frac{\pi}{2} + 2k\pi, k \in \mathbb{Z} \right\},$$

and the optimal value is  $F^* = \frac{n(C-2a)^2}{1+n}$ . This example satisfies all the assumptions of BVFSM, but does not meet the LLC assumption in [27], [9], [28], which makes it a good example to validate the advantages of BVFSM.

We compare the proposed algorithm with several gradient-based optimization methods, including RHG, BDA, CG and Neumann. Note that they all assume the solution of the LL problem is unique except BDA, so we directly regard the obtained local optimal solutions as the unique solutions of LL problems for these methods. We set  $T = 100$  for RHG and BDA,  $T = 100$ ,  $Q = 20$  for CG and Neumann, the aggregation parameters equal to 0.5 in BDA, and  $(\mu_k, \theta_k, \sigma_k^{(1)}) = (1.0, 1.0, 1.0)/1.01^k$ ,  $\sigma_k^{(2)} = f(x, y) + n$ , step size  $\alpha = 0.01$ ,  $T_x = 50$ ,  $T_y = 25$ , and  $L = 1$  in BVFSM.

Figure 1 compares the convergence curves of the UL variable  $x$  and the function value  $F(x, y)$  in the 2-dimensional case ( $n = 2$ ). Note that in this situation, the optimal solution is  $(x, y) = (-2/3 + \pi, 8/3 + \pi/2, 8/3 + \pi/2)$ . In order to better show the impact of initial points, we also set different initial points for all methods. From Figure 1, firstly, when the initial point is  $(x, y) = (8, 8, 8)$ , existing methods show the trend of convergence at the initial stage of the iteration, but they soon stop further convergence due to falling into a local optimal solution. Furthermore, when the initial point is  $(x, y) = (0, 0, 0)$ , existing methods show a trend away from the optimal solution during the whole iterative process and cannot converge. On the contrary, our method can converge to the optimal solution under different initial points. To better verify the influence of LL dimension  $n$  on the results, we also test the performance by various methods for larger-scale problems in Table 4. The experiment shows that our method can still maintain good convergence performance with high-

TABLE 4  
The errors of UL variable  $\|x - x^*\|/\|x^*\|$  using gradient-based BLO algorithms with large-scale LL of  $n$  dimension.

$n$	RHG	BDA	CG	Neumann	BVFSM
50	2.296	2.336	2.058	2.260	<b>0.117</b>
100	2.253	2.294	2.073	2.236	<b>0.159</b>
150	2.213	2.253	2.032	2.202	<b>0.190</b>
200	2.187	2.227	1.972	2.178	<b>0.209</b>

TABLE 5  
Comparison of the computation time (seconds, S) for each step of calculating the gradient of  $x$  among BVFSM and existing gradient-based methods under various scales  $n$  and  $m$ . N/A means that the calculation time exceeds 3600 seconds.

(a)  $m = 1$

$n$	RHG	BDA	CG	Neumann	BVFSM
1	0.063	0.124	0.033	0.063	<b>0.016</b>
10	0.469	0.879	0.319	0.471	<b>0.063</b>
100	5.995	7.014	4.467	4.802	<b>0.581</b>
1000	114.7	116.8	78.01	77.03	<b>4.416</b>
10000	2015	2037	1652	1602	<b>62.51</b>
15000	N/A	N/A	3173	2838	<b>80.95</b>
20000	N/A	N/A	N/A	N/A	<b>132.6</b>

(b)  $m = 100$

$n$	RHG	BDA	CG	Neumann	BVFSM
1	0.067	0.131	0.035	0.066	<b>0.019</b>
10	0.495	0.926	0.335	0.497	<b>0.073</b>
100	6.353	7.377	4.728	5.057	<b>0.674</b>
1000	120.5	122.9	81.94	81.06	<b>5.106</b>
10000	2134	2147	1736	1691	<b>72.02</b>
15000	N/A	N/A	3352	2982	<b>93.80</b>
20000	N/A	N/A	N/A	N/A	<b>152.5</b>

(c)  $m = 1000$

$n$	RHG	BDA	CG	Neumann	BVFSM
1	0.077	0.151	0.042	0.076	<b>0.021</b>
10	0.574	1.070	0.388	0.573	<b>0.084</b>
100	7.353	8.492	5.439	5.833	<b>0.775</b>
1000	138.9	141.7	94.93	93.50	<b>5.978</b>
10000	2466	2485	2006	1951.6	<b>83.24</b>
15000	N/A	N/A	N/A	3447	<b>108.3</b>
20000	N/A	N/A	N/A	N/A	<b>176.4</b>

dimensional LL, while existing methods fail because they cannot solve the non-convex LL with convergence guarantee.

Table 5 compares the computation time among problems of various scales. Note that the scale-up of UL variable can be

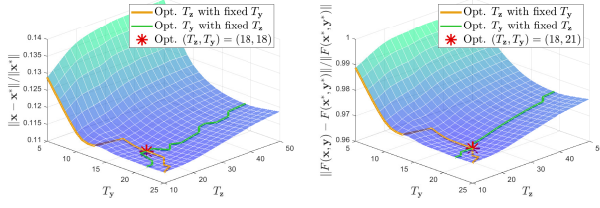
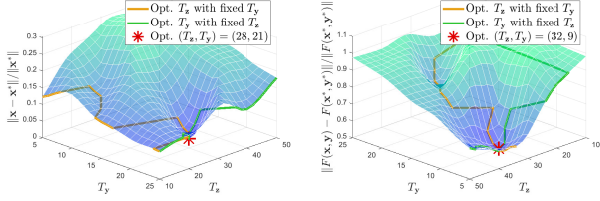
(a) Errors when  $\mu_0, \theta_0 = 0.01$ (b) Errors when  $\mu_0, \theta_0 = 0.001$ 

Fig. 2. Illustration of the errors of iteration solutions under different settings of specified  $T_z$ ,  $T_y$ ,  $\mu$  and  $\theta$ . Here  $T_z$  and  $T_y$  are the number of iterations for gradient descent on sub-problems in Eq. (10) and Eq. (11), which affect the accuracy of obtained solution. The curves on the surfaces denote the optimal  $T_z$  (or  $T_y$ ) to minimize the error with fixed  $T_y$  (or  $T_z$ ). Subfigure (a) shows that the increasing of  $T_y$  and  $T_z$  abnormally leads to the deviation of the solution, because with larger regularization coefficients  $\mu$  and  $\theta$ , the regularized problems are away from the original problems. Subfigure (b) shows that smaller regularization coefficients may not completely overcome the ill condition of the LL problem, resulting in the instability of the surfaces.

achieved by converting the one-dimensional  $\mathbf{x}$  to the mean of multi-dimensional  $\mathbf{x}$ . As we can see, our method costs the least computation time for problems of all scales, and the size  $n$  of LL variable has much more influence than the size  $m$  of UL variable. This allows us to apply it to more complex LL problems, which existing methods cannot deal with. We further explore the performance of our method on LL problems containing complex network structures in Section 5.2.

In Figure 2, we compare the performance under different settings. We analyze the impact of  $T_z$  and  $T_y$  respectively, on the convergence results for varied regularization coefficients  $\mu$  and  $\theta$ .  $T_z$  and  $T_y$  are the number of iterations for gradient descent on LL sub-problems in Eq. (10) and simple BLO problems in Eq. (11), which affect the accuracy of the obtained solution. Figure 2(a) shows that the increasing of  $T_y$  and  $T_z$  abnormally leads to the deviation of the solution, since with larger regularization coefficients  $\mu$  and  $\theta$ , the regularized problems are away from the original problems. Figure 2(b) shows that smaller regularization coefficients may not completely overcome the ill condition of the LL problem, which means the small coefficients cause the approximate problem to remain a little ill-conditioned, resulting in the instability of the surfaces. Hence, it is not an easy task to determine the regularization coefficients. Since the selection of such parameters is often highly related to the specific problem, in order to maintain the fairness for comparing the computational burden with existing methods, we set  $T_z + 2T_y = T$  (because we need to calculate the gradient of two functions  $F$  and  $f$  for a  $T_y$ -step gradient descent) in all experiments.

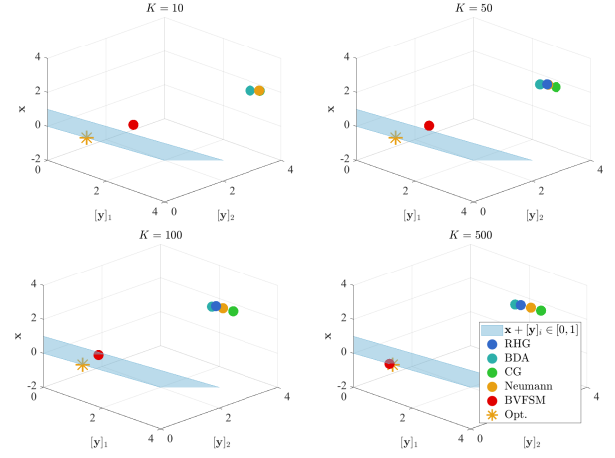
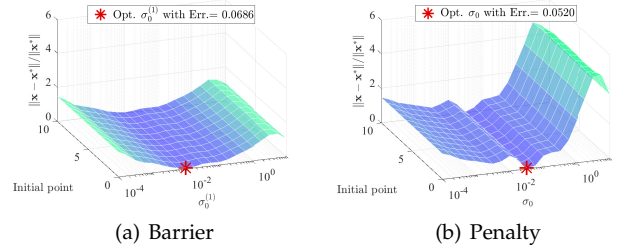


Fig. 3. Illustration of the relationship between the true optimal solution (“Opt.” for short) and the solutions obtained by different methods during the UL iteration for constrained BLO. It can be seen that BVFSM can gradually converge to the optimal point inside the feasible region, while other methods cannot deal with the constraint at all. The legend is only plotted in the last subfigure.



(a) Barrier

(b) Penalty

Fig. 4. The convergence behavior of BVFSM about UL variable  $\mathbf{x}$  under different initial points and parameters with (a) barrier and (b) penalty functions respectively. Err. in the legend denotes  $\|\mathbf{x} - \mathbf{x}^*\|/\|\mathbf{x}^*\|$ . We select the truncated log barrier and quadratic penalty as the representatives of barrier and penalty functions respectively. Choosing the barrier function leads to higher stability and less sensitivity to parameters, while using the penalty function is more sensitive to parameters but can obtain smaller errors. At the same time, both methods are insensitive to initial values.

To show the performance of our BVFSM when applied to problems with constraints as discussed in Section 3.3, we use the following constrained example with non-convex LL:

$$\begin{aligned} \min_{\mathbf{x} \in \mathbb{R}, \mathbf{y} \in \mathbb{R}^n} & \quad \|\mathbf{x} - \mathbf{a}\|^2 + \|\mathbf{y} - \mathbf{a}\|^2 \\ \text{s.t. } & \quad [\mathbf{y}]_i \in \arg \min_{[\mathbf{y}]_i \in \mathbb{R}} \left\{ \sin(\mathbf{x} + [\mathbf{y}]_i - [\mathbf{c}]_i) : \mathbf{x} + [\mathbf{y}]_i \in [0, 1] \right\}, \forall i, \end{aligned}$$

where  $\mathbf{a} \in \mathbb{R}$  and  $\mathbf{c} \in \mathbb{R}^n$  are any fixed given constant and vector such that  $[\mathbf{c}]_i \in [0, 1]$  for any  $i = 1, \dots, n$ . The solution is

$$\mathbf{x} = \frac{1-n}{1+n}\mathbf{a}, \text{ and } [\mathbf{y}]_i = -\mathbf{x}, \forall i,$$

and the optimal value is  $F^* = \frac{4n}{1+n}\mathbf{a}^2$ .

We conduct the experiment under the 2-dimensional case ( $n = 2$ ) and set  $\mathbf{a} = 2$  and  $[\mathbf{c}]_i = 1$ , for any  $i = 1, 2, \dots, n$ . The constraint is carried out via  $(\mathbf{x} + [\mathbf{y}]_i - 0.5)^2 - 0.25 \leq 0$ , for each component of  $\mathbf{y}$ , which is equivalent to  $\mathbf{x} + [\mathbf{y}]_i \in [0, 1]$ . Figure 3 compares the solutions obtained by various methods. It can be seen that when dealing with constrained LL problems, only our proposed method can effectively deal

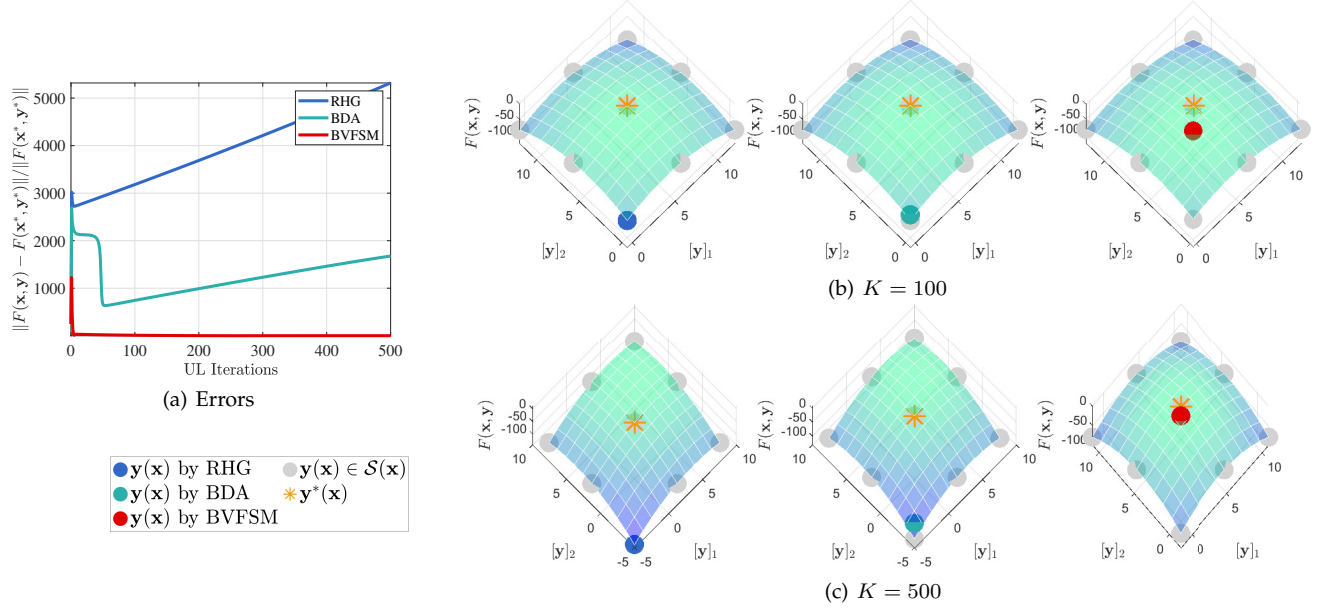


Fig. 5. An evaluation of the convergence behavior about UL objective in pessimistic BLO. We compare our BVFSM with other gradient-based BLO algorithm (RHG and BDA). Errors in subfigure (a) denotes  $\|F(\mathbf{x}, \mathbf{y}) - F(\mathbf{x}^*, \mathbf{y}^*)\| / \|F(\mathbf{x}^*, \mathbf{y}^*)\|$ . On the right side, we show the LL solution  $\mathbf{y}(\mathbf{x})$  obtained by different methods. Subfigures (b) and (c) illustrate the results when  $K = 100$  and  $K = 500$ , respectively. Here the surfaces denote  $F(\mathbf{x}, \mathbf{y})$ , and  $\mathbf{y}^*(\mathbf{x})$  means the true LL solution for a fixed UL variable  $\mathbf{x}$ . We can find that both RHG and BDA choose the incorrect solutions of LL problem in the pessimistic situation, while BVFSM correctly choose the LL solution.

with constraints and converge to the true solution inside the feasible set. Therefore, our method has broader application space, and we will discuss the experiment in real learning tasks in Section 5.2, which solves problems with constraints on the UL.

For comparing the performance of different auxiliary functions, we try barrier and penalty functions for  $P_{H, \sigma_H}$ ,  $P_{h, \sigma_h}$  and  $P_{f, \sigma_f}$ , which can be selected arbitrarily and separately indeed, but here are chosen the same to be compared more directly. Since all of these auxiliary functions can guarantee the convergence theoretically, we mainly focus on the robustness of them under different settings. Figure 4 shows the eventual convergence results under different initial points and coefficients. It can be seen that using a penalty function can converge only under certain settings within a small region, while using a barrier function has greater robustness, so we use barrier functions in future experiments. In Section 5.2, we further show investigations on penalty and barrier functions on complex networks.

To study the performance of pessimistic BLO, we simply change  $\min_{\mathbf{x} \in \mathbb{R}, \mathbf{y} \in \mathbb{R}^n}$  to  $\min_{\mathbf{x} \in \mathbb{R}} \max_{\mathbf{y} \in \mathbb{R}^n}$  and  $\|\mathbf{x} - \mathbf{a}\|^2 + \|\mathbf{y} - \mathbf{a} - \mathbf{c}\|^2$  to  $\|\mathbf{x} - \mathbf{a}\|^2 - \|\mathbf{y} - \mathbf{a} - \mathbf{c}\|^2$  in Eq. (20), which is similar to the above optimistic BLO example and has the same optimal solution. As the representatives of methods with or without unique LL solution, we select RHG and BDA respectively for comparison. We make no adaptive modifications to these methods which do not consider the pessimistic BLO situation. The experiment is also conducted under the 2-dimensional case ( $n = 2$ ).

In Figure 5, we show the iteration curves of UL objective and how various methods choose  $\mathbf{y} \in \mathcal{S}(\mathbf{x})$  when  $\mathcal{S}(\mathbf{x})$  is not a singleton. It can be seen from Figure 5(a) that our method has significantly better convergence to the optimal solution than other methods on the pessimistic BLO problem, while RHG and BDA cannot converge at all. As shown in

Figure 5(b) and 5(c), this is because in the pessimistic case, existing methods cannot correctly select the optimal solution in the LL solution set, resulting in the divergence of results.

## 5.2 Hyper-parameter Optimization

In this subsection, we use a specific task of hyper-parameter optimization, called data hyper-cleaning, to evaluate the performance of BVFSM when the LL problem is non-convex. Assuming that some of the labels in our dataset are contaminated, the goal of data hyper-cleaning is to reduce the impact of incorrect samples by adding hyper-parameters to them.

In the experiment, we set  $\mathbf{y} \in \mathbb{R}^{10 \times 301} \times \mathbb{R}^{300 \times d}$  as the parameter of a non-convex 2-layer linear network classifier where  $d$  is the dimension of data, and  $\mathbf{x} \in \mathbb{R}^{|\mathcal{D}_{tr}|}$  as the weight of each sample in the training set. Therefore, the LL problem is to learn a classifier  $\mathbf{y}$  by cross-entropy loss  $g$  weighted with given  $\mathbf{x}$ :

$$f(\mathbf{x}, \mathbf{y}) = \sum_{(\mathbf{u}_i, \mathbf{v}_i) \in \mathcal{D}_{tr}} [\text{sigmoid}(\mathbf{x})]_i g(\mathbf{y}, \mathbf{u}_i, \mathbf{v}_i),$$

where  $(\mathbf{u}_i, \mathbf{v}_i)$  are the training samples,  $\text{sigmoid}(\mathbf{x})$  denotes the sigmoid function on  $\mathbf{x}$  to constrain the weights to the range of  $[0, 1]$ , and  $g$  is the cross-entropy loss. The UL problem is to find a weight  $\mathbf{x}$  which can reduce the cross-entropy loss  $g$  of  $\mathbf{y}$  on a cleanly labeled validation set:

$$F(\mathbf{x}, \mathbf{y}) = \sum_{(\mathbf{u}_i, \mathbf{v}_i) \in \mathcal{D}_{val}} g(\mathbf{y}, \mathbf{u}_i, \mathbf{v}_i).$$

In addition, we also consider adding explicit constraints directly on  $\mathbf{x}$  (as discussed in Section 3.3) instead of using the sigmoid function as indirect constraints. The constraint is carried out via  $([\mathbf{x}]_i - 0.5)^2 - 0.25 \leq 0$ , for each component of  $\mathbf{x}$ , such that  $[\mathbf{x}]_i \in [0, 1]$ .

Our experiment is based on MNIST, FashionMNIST [48] and CIFAR10 datasets. For each dataset, we randomly select



TABLE 6

Comparison among existing methods, BVFSM, and BVFSM with constraints (BVFSM-C) for data hyper-cleaning tasks on MNIST, FashionMNIST and CIFAR10. The F1 score is the harmonic mean of precision and recall.

Method	MNIST			FashionMNIST			CIFAR10		
	Acc.	F1 score	Time (S)	Acc.	F1 score	Time (S)	Acc.	F1 score	Time (S)
RHG	87.90	89.36	0.4131	81.91	87.12	0.4589	34.95	68.27	1.3374
TRHG	88.57	89.77	0.2623	81.85	86.76	0.2840	35.42	68.06	0.8409
CG	89.19	85.96	0.1799	83.15	85.13	0.2041	34.16	69.10	0.4796
Neumann	87.54	89.58	0.1723	81.37	87.28	0.1958	33.45	68.87	0.4694
BDA	87.15	90.38	0.6694	79.97	88.24	0.8571	36.41	67.33	1.4869
BVFSM	90.41	91.19	<b>0.1480</b>	<b>84.31</b>	88.35	0.1612	<b>38.19</b>	69.55	<b>0.4092</b>
BVFSM-C	<b>90.94</b>	<b>91.83</b>	0.1566	83.23	<b>89.74</b>	<b>0.1514</b>	37.33	<b>69.73</b>	0.4374

TABLE 7

Comparison of the computing memory (VRAM) and time among BVFSM and existing gradient-based methods in networks of different scales for data hyper-cleaning. Regardless of the time limit, here N/A means it is unable to compute due to the 8GB VRAM limitation. BVFSM maintains the minimal computational burden and the fastest computational speed for large-scale LL problems.

(a) 2-layer

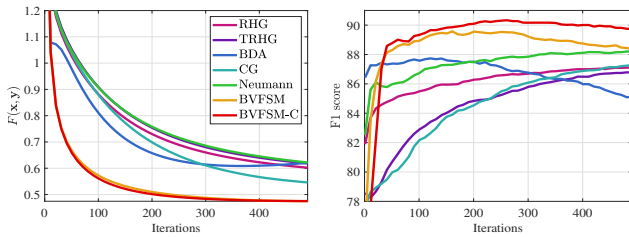
Width	Memory (MB)					Time (S)				
	RHG	BDA	CG	Neumann	BVFSM	RHG	BDA	CG	Neumann	BVFSM
50	347	617	244	209	<b>65</b>	0.3499	0.6563	0.1756	0.1870	<b>0.1179</b>
100	572	1052	402	344	<b>68</b>	0.3594	0.6401	0.1751	0.1679	<b>0.1252</b>
150	760	1413	534	458	<b>72</b>	0.3557	0.6056	0.1785	0.1765	<b>0.1319</b>
200	1003	1885	705	604	<b>75</b>	0.3643	0.6236	0.1826	0.1775	<b>0.1421</b>

(b) 5-layer

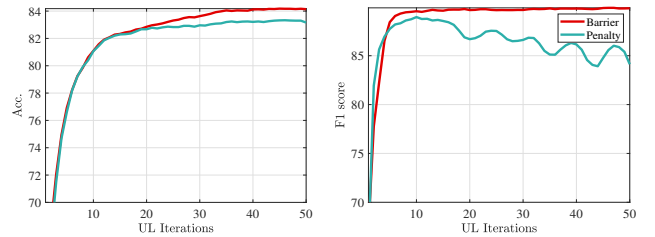
Width	Memory (MB)					Time (S)				
	RHG	BDA	CG	Neumann	BVFSM	RHG	BDA	CG	Neumann	BVFSM
50	923	1770	649	556	<b>74</b>	0.7057	1.4875	0.3587	0.3449	<b>0.2236</b>
100	1784	3471	1255	1075	<b>87</b>	0.7081	1.7982	0.3584	0.3453	<b>0.2229</b>
150	2504	4883	1761	1509	<b>99</b>	0.7528	1.9365	0.3698	0.3573	<b>0.2432</b>
200	3451	N/A	2427	2080	<b>114</b>	0.9642	N/A	0.4492	0.4545	<b>0.2780</b>

(c) 10-layer

Width	Memory (MB)					Time (S)				
	RHG	BDA	CG	Neumann	BVFSM	RHG	BDA	CG	Neumann	BVFSM
50	1883	3691	1324	1135	<b>89</b>	1.3202	3.7299	0.6879	0.6584	<b>0.3997</b>
100	3804	N/A	2676	2293	<b>118</b>	1.2678	N/A	0.6496	0.6407	<b>0.3993</b>
150	5410	N/A	3805	3261	<b>144</b>	1.5186	N/A	0.7358	0.7188	<b>0.4311</b>
200	N/A	N/A	N/A	N/A	<b>177</b>	N/A	N/A	N/A	N/A	<b>0.5023</b>

(a) UL objective value  $F(\mathbf{x}, \mathbf{y})$ 

(b) F1 score



(a) Accuracy

(b) F1 score

Fig. 6. The value of UL objective  $F(\mathbf{x}, \mathbf{y})$  and F1 score using different gradient-based methods for data hyper-cleaning. The curves are based on the FashionMNIST experiment in Table 6. The legend is only plotted in subfigure (a).

5000 samples as the training set  $\mathcal{D}_{\text{tr}}$ , 5000 samples as the validation set  $\mathcal{D}_{\text{val}}$ , and 10000 samples as the test set  $\mathcal{D}_{\text{test}}$ . After that, we contaminated half of the labels in  $\mathcal{D}_{\text{tr}}$ .

Table 6 shows the accuracy, F1 score and calculation time of the compared methods and BVFSM on three different datasets. From the result, BVFSM achieves the most competitive performance in accuracy and F1 score on all datasets.

Fig. 7. Obtained accuracy and F1 score with barrier and penalty functions for data hyper-cleaning. The curves are based on the FashionMNIST experiment. We choose the truncated log barrier and quadratic penalty as the representatives of barrier and penalty functions respectively. It can be seen that using a barrier function is better than penalty in higher accuracy and greater stability of F1 score. The legend is only plotted in subfigure (b).

Furthermore, BVFSM is faster than EGBMs and IGBMs, and this advantage is more evident in CIFAR10 datasets with larger dimension of the LL variable, consistent with the complexity analysis given in Section 4.2. The values of UL objective and F1 scores of BVFSM and compared methods on the FashionMNIST dataset are also plotted in Figure 6.

As for the performance of BLO with constraints, we can find from Table 6 that BVFSM with constraints (denoted as BVFSM-C in Table 6) has slightly lower accuracy but higher F1 score than BVFSM using sigmoid function without explicit constraints. This is because for BVFSM without constraints, the compound of sigmoid function in the objective decreases the derivative with respect to  $\mathbf{x}$ , and thus the UL variable  $\mathbf{x}$  with small change rate contributes to the slow convergence. Therefore, BVFSM with constraints performs slightly worse in the accuracy of representing the convergence of the LL variable, but better in the F1 score which reflects the convergence of the UL variable.

For comparing the performance of different auxiliary functions, we show the effect of barrier and penalty functions on the accuracy and F1 score in Figure 7. We can find that, consistent with the numerical example in Figure 4, the barrier function performs better without the need for too much fine tuning of parameters.

We further show the impact of network structures in width and depth on computing time in Table 7. For the LL variable  $\mathbf{y}$  of different scales, we use fully connected networks of 2-layer, 5-layer and 10-layer, and four network widths of 50, 100, 150 and 200 respectively. It is worth noting that the computational burden of all methods is not quite sensitive to the network width, but very sensitive to the network depth. With the deepening of the network, existing methods have collapsed in varying degrees due to occupying too much memory, while our method can always keep the computation stable. Since there is no need to retain the iteration trajectory of the LL problem, the storage burden of our method is much less than that of EGBMs. Thanks to the fact that our method does not need to calculate the Jacobian- and Hessian-vector products (realized by saving an additional calculation graph in AD), the storage burden is also significantly lower than that of IGBMs.

In addition, we verify our computing burden on large-scale networks closer to real applications such as the VGG16 network on CIFAR10 dataset. Because VGG16 has too much computational burden on the existing methods, in order to make them work, we change the experimental setting as follows. For each dataset, we randomly select 4096 samples as the training set  $\mathcal{D}_{\text{tr}}$ , 4096 samples as the validation set  $\mathcal{D}_{\text{val}}$ , and 512 samples as the test set  $\mathcal{D}_{\text{test}}$ . Because the original network is too computationally intensive for EGBMs, we perform an additional experiment on some sufficiently small batch size and iteration number  $T$ . We also simplify the convolution layers from 13 layers in VGG16 to only the first two layers, and retain the last 3 linear layers, to compare with other methods which lead to heavy computational burden.

As shown in Table 8, our method always has the fastest computation speed under various settings. Besides, our method still works well with a large  $T$  and batch size. We attribute these superior results to our novel way of solving the optimization problem with the re-characterization via value-function.

### 5.3 Few-shot Learning

We then conduct experiments to verify the performance of BVFSM on the task of few-shot learning. Few-shot learning is one of the most popular applications in meta-learning, whose

TABLE 8

Comparison of the computing time (seconds) for each epoch among BVFSM and existing gradient-based methods for data hyper-cleaning in VGG series networks with different convolution layers (Conv.), batch sizes (B) and  $T$ . N/A means it is unable to compute due to the memory limitation. Notice that a smaller batch size may take more computation time because the batch switching time increases. BVFSM maintains the minimal computational burden and the fastest computational speed, especially when the LL problem is large-scale in real-world networks.

Conv.	(B,T)	RHG	CG	Neumann	BVFSM
2	(1,7)	7515	4730	3225	<b>2252</b>
2	(128,20)	N/A	N/A	415.4	<b>60.81</b>
13	(128,100)	N/A	N/A	472.9	<b>171.9</b>
13	(512,100)	N/A	N/A	N/A	<b>121.8</b>

goal is to learn an algorithm that can also handle new tasks well. Specifically, each task is an  $N$ -way classification and it aims to learn the hyper-parameter  $\mathbf{x}$  so that each task can be solved by only  $M$  training samples (i.e.,  $N$ -way  $M$ -shot).

Similar to recent works [8], [29], [30], we model the network with two parts: a four-layer convolution network  $\mathbf{x}$  as a common feature extraction layer among different tasks, and a logical regression layer  $\mathbf{y} = \mathbf{y}^i$  as the separated classifier for each task. We also set dataset as  $\mathcal{D} = \{\mathcal{D}^i\}$ , where  $\mathcal{D}^i = \mathcal{D}_{\text{tr}}^i \cup \mathcal{D}_{\text{val}}^i$  for the  $i$ -th task. Then we set the loss function of the  $i$ -th task to be cross-entropy  $g(\mathbf{x}, \mathbf{y}^i; \mathcal{D}_{\text{tr}}^i)$  for the LL problem, and thus the LL objective can be defined as

$$f(\mathbf{x}, \mathbf{y}) = \sum_i g(\mathbf{x}, \mathbf{y}^i; \mathcal{D}_{\text{tr}}^i).$$

As for the UL objective, we also utilize the cross-entropy function but define it based on  $\{\mathcal{D}_{\text{val}}^i\}$  as

$$F(\mathbf{x}, \mathbf{y}) = \sum_i g(\mathbf{x}, \mathbf{y}^i; \mathcal{D}_{\text{val}}^i).$$

Our experiment is performed on the widely used benchmark dataset: Omniglot [49], which contains examples of 1623 different handwritten characters from 50 alphabets.

We compare our BVFSM with several approaches, such as MAML, Meta-SGD, Reptile, iMAML, RHG, TRHG and BDA [29], [30]. It can be seen in Table 9 that BVFSM achieves slightly poorer performance than existing methods in the 5-way task. This is because when dealing with small-scale LLC problems, the strength of regularization term by BVFSM to accelerate the convergence cannot fully counteract its impact on the offset of the solution. However, for more complex LL problems of larger-scale (such as 20-way, 30-way and 40-way), thanks to the regularization term, BVFSM reveals significant advantages over other methods.

### 5.4 Generative Adversarial Networks

Here we perform experiments on GAN to illustrate the application of BVFSM for pessimistic BLO problems. In order to demonstrate the effect of our method intuitively, we train a simple GAN architecture on a 2D mixture of 8 Gaussians arranged on a circle.

To be specific, GAN is a network used for unsupervised machine learning to build a min-max game between two players, i.e., the generator  $\text{Gen}(\mathbf{x}; \cdot)$  with the network parameter  $\mathbf{x}$ , and the discriminator  $\text{Dis}(\mathbf{y}; \cdot)$  with the network parameter  $\mathbf{y}$ . We denote the standard Gaussian distribution as  $\mathcal{N}(0, 1)$  and the real data distribution as  $p_{\text{data}}$ . The generator  $\text{Gen}$

TABLE 9

Averaged accuracy using various methods (including model-based methods and gradient-based BLO methods) for few-shot classification problems (1- and 5-shot, i.e.,  $M = 1, 5$ , and  $N = 5, 20, 30, 40$ ) on Omniglot.

Method	5-way		20-way		30-way		40-way	
	1-shot	5-shot	1-shot	5-shot	1-shot	5-shot	1-shot	5-shot
MAML	98.70	<b>99.91</b>	95.80	98.90	86.86	96.86	85.98	94.46
Meta-SGD	97.97	98.96	93.98	98.42	89.91	96.21	87.39	95.10
Reptile	97.68	99.48	89.43	97.12	85.40	95.28	82.50	92.79
iMAML	<b>99.16</b>	99.67	94.46	98.69	89.52	96.51	87.28	95.27
RHG	98.64	99.58	96.13	99.09	93.92	98.43	90.78	96.79
T-RHG	98.74	99.71	95.82	98.95	94.02	98.39	90.73	96.79
BDA	99.04	99.74	96.50	<b>99.19</b>	94.37	98.53	92.49	97.12
BVFSM	98.85	99.21	<b>96.73</b>	98.95	<b>94.65</b>	<b>98.56</b>	<b>92.73</b>	<b>97.61</b>

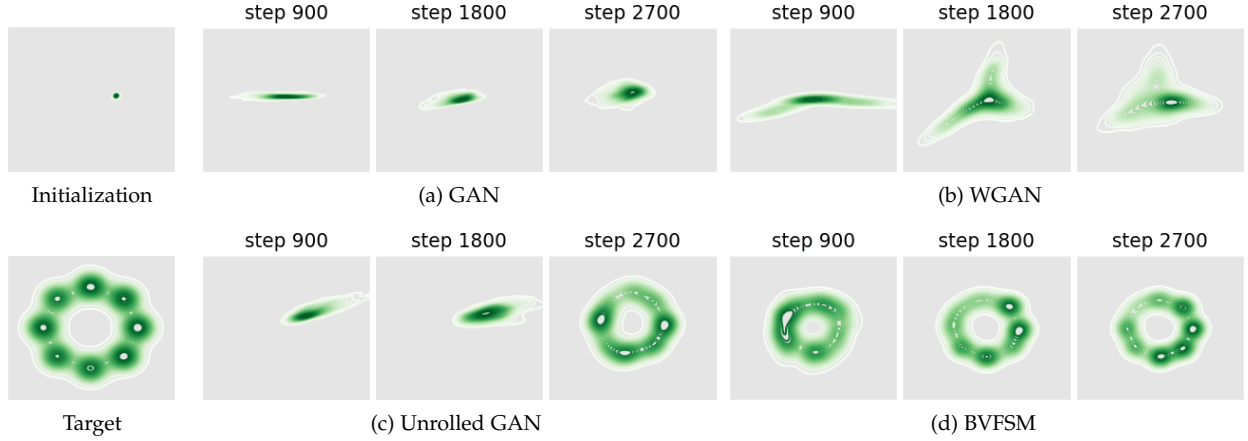


Fig. 8. Comparison of GAN training on a toy 2D mixture of Gaussians dataset. We show the heat map of the generated distribution as the number of training steps increases. Subfigure (a) indicates vanilla GAN can capture only one distribution, while in subfigure (b), WGAN attempts to capture all distributions at the same time with one Gaussian distribution, but fails to achieve satisfactory performance. Unrolled GAN in subfigure (c) can approximate all distributions simultaneously with the help of a leader-follower structure, but lacks further details. In contrast, our BVFSM fits all Gaussian distributions well with plenty of details, as shown in subfigure (d).

tries to fool  $\text{Dis}$  by producing data from random latent vector  $\mathbf{v} \sim \mathcal{N}(0, 1)$ , while the discriminator  $\text{Dis}$  distinguishes between real data  $\mathbf{u} \sim p_{\text{data}}$  and generated data  $\text{Gen}(\mathbf{x}; \mathbf{v})$  by outputting the probability that the samples are real. The goal of GAN is to  $\min_{\mathbf{v}} \max_{\mathbf{u}} -\log(\text{Dis}(\mathbf{y}; \mathbf{u})) - \log(1 - \text{Dis}(\mathbf{y}; \text{Gen}(\mathbf{x}; \mathbf{v})))$  [50].

However, this traditional modeling method regards  $\text{Dis}$  and  $\text{Gen}$  as equal status, and does not characterize the leader-follower relationship that  $\text{Gen}$  first generates data and after that  $\text{Dis}$  judges the data, which can be modeled by Stackelberg game and captured through BLO problems. Specifically, from this perspective, generative adversarial learning corresponds to a pessimistic BLO problem: the UL objective  $F$  of  $\text{Gen}$  tries to generate adversarial samples, and the LL objective  $f$  of  $\text{Dis}$  aims to learn a robust classifier which can maximize the UL objective. Therefore, we reformulate GAN into the form in Eq. (15) discussed in Section 3.4 to model this relationship, and call it bi-level GAN. Concretely, for the follower  $\text{Dis}(\mathbf{y}; \cdot)$ , the LL objective is consistent with the original GAN:

$$f(\mathbf{x}, \mathbf{y}) = \log(\text{Dis}(\mathbf{y}; \mathbf{u})) + \log(1 - \text{Dis}(\mathbf{y}; \text{Gen}(\mathbf{x}; \mathbf{v}))).$$

As for the UL, considering the antagonistic goals of  $\text{Gen}$  and  $\text{Dis}$ , we model the UL problem as

$$F(\mathbf{x}, \mathbf{y}) = \log(\text{Dis}(\mathbf{y}; \text{Gen}(\mathbf{x}; \mathbf{v}))).$$

Note that the popular WGAN [51] is a variation of the most classic vanilla GAN [50] (or simply GAN), while unrolled GAN [11] and the GAN generated by our BVFSM belong to bi-level GAN, modeling from a BLO perspective. Our method has the following two advantages over other types of GAN. On the one hand, compared with vanilla GAN and WGAN, bi-level GAN can effectively model the leader-follower relationship between the generator and discriminator, rather than regard them as the same status. On the other hand, in bi-level GAN, our method considers the situation that the objective has multiple solutions, from the viewpoint of pessimistic BLO, with theoretical convergence guarantee, which unrolled GAN cannot achieve.

The dataset in this experiment is sampled from a mixture of 8 Gaussians with standard deviation 0.02. The 8 points corresponding to the means are equally spaced around a circle of radius 2. The generator consists of a fully-connected network with 2 hidden layers of size 128 with ReLU activation followed by a linear projection to 2 dimensions. The discriminator first scales its input down by a factor of 4 (to roughly scale it to  $(-1, 1)$ ), and is followed by a 1-layer fully-connected network from ReLU activation to a linear layer of size 1 to act as the logit.

As shown in Figure 8, we present a visual comparison of sample generation among GAN, WGAN, unrolled GAN, and our method. It can be seen that vanilla GAN can capture only one distribution rather than all Gaussian distributions at a



TABLE 10

Comparison of the KL divergence by various GAN. The divergence between the generated and target distribution by BVFSM is the smallest.

	GAN	WGAN	Unrolled GAN	BVFSM
KL Divergence	2.56	2.48	0.26	<b>0.15</b>

time, because it ignores the leader-follower structure. WGAN benefits from the improvement of distance function and uses one distribution to approximate all Gaussian distributions at the same time, but it fails to display satisfying performance. Thanks to the leader-follower modeling by BLO, unrolled GAN shows the ability to capture all distributions simultaneously, but it lacks further details of the distribution. However, the desirable treatment of non-convex problems by BVFSM brings about its ability to fit all distributions well with details.

In addition, we show the KL divergence between the generated and target image in Table 10. It can be seen that the traditional alternately optimized GAN and WGAN yield larger KL divergence, while unrolled GAN and our method, which consider GAN as a BLO model, produce smaller KL divergence, and our method further achieves the best result.

## 6 CONCLUSIONS

In this paper, we propose a novel bi-level algorithm BVFSM to remove the LLC condition required by earlier works, and improve the efficiency of gradient-based method, to break through the bottleneck caused by high-dimensional non-convex LL problems of complex real-world tasks. By transforming the regularized LL problem into UL objective by the value-function-based sequential minimization method, we obtain a sequence of single-level unconstrained differentiable problems to approximate the original problem. We prove the convergence without LLC, and present our numerical superiority through complexity analysis and numerical evaluations for a variety of applications. We also extend our method to BLO problems with constraints, and pessimistic BLO problems.

## ACKNOWLEDGMENTS

This work is partially supported by the National Natural Science Foundation of China (Nos. 61922019, 61733002 and 11971220), Liaoning Revitalization Talents Program (No. XLYC1807088), the Fundamental Research Funds for the Central Universities, Shenzhen Science and Technology Program (No. RCYX20200714114700072), and Guangdong Basic and Applied Research Foundation (No. 2019A1515011152).

## REFERENCES

- [1] R. Liu, X. Liu, X. Yuan, S. Zeng, and J. Zhang, "A value-function-based interior-point method for non-convex bi-level optimization," in *ICML*, 2021.
- [2] L. Franceschi, M. Donini, P. Frasconi, and M. Pontil, "Forward and reverse gradient-based hyperparameter optimization," in *ICML*, 2017.
- [3] T. Okuno, A. Takeda, and A. Kawana, "Hyperparameter learning via bilevel nonsmooth optimization," *arXiv preprint arXiv:1806.01520*, 2018.
- [4] M. Mackay, P. Vicol, J. Lorraine, D. Duvenaud, and R. Grosse, "Self-tuning networks: Bilevel optimization of hyperparameters using structured best-response functions," in *ICLR*, 2018.
- [5] H. Liu, K. Simonyan, and Y. Yang, "DARTS: differentiable architecture search," in *ICLR*, 2019.
- [6] H. Liang, S. Zhang, J. Sun, X. He, W. Huang, K. Zhuang, and Z. Li, "Darts+: Improved differentiable architecture search with early stopping," *arXiv preprint arXiv:1909.06035*, 2019.
- [7] X. Chen, L. Xie, J. Wu, and Q. Tian, "Progressive differentiable architecture search: Bridging the depth gap between search and evaluation," in *ICCV*, 2019.
- [8] L. Franceschi, P. Frasconi, S. Salzo, R. Grazzi, and M. Pontil, "Bilevel programming for hyperparameter optimization and meta-learning," in *ICML*, 2018.
- [9] A. Rajeswaran, C. Finn, S. M. Kakade, and S. Levine, "Meta-learning with implicit gradients," in *NeurIPS*, 2019.
- [10] D. Zügner and S. Günnemann, "Adversarial attacks on graph neural networks via meta learning," in *ICLR*, 2019.
- [11] L. Metz, B. Poole, D. Pfau, and J. Sohl-Dickstein, "Unrolled generative adversarial networks," *arXiv preprint arXiv:1611.02163*, 2016.
- [12] D. Pfau and O. Vinyals, "Connecting generative adversarial networks and actor-critic methods," *arXiv preprint arXiv:1610.01945*, 2016.
- [13] Z. Yang, Y. Chen, M. Hong, and Z. Wang, "Provably global convergence of actor-critic: A case for linear quadratic regulator with ergodic cost," in *NeurIPS*, 2019.
- [14] R. Liu, S. Cheng, Y. He, X. Fan, Z. Lin, and Z. Luo, "On the convergence of learning-based iterative methods for nonconvex inverse problems," *IEEE TPAMI*, 2019.
- [15] R. Liu, Z. Li, Y. Zhang, X. Fan, and Z. Luo, "Bi-level probabilistic feature learning for deformable image registration," in *IJCAI*, 2020.
- [16] R. Liu, J. Liu, Z. Jiang, X. Fan, and Z. Luo, "A bilevel integrated model with data-driven layer ensemble for multi-modality image fusion," *IEEE TIP*, 2020.
- [17] R. Liu, P. Mu, J. Chen, X. Fan, and Z. Luo, "Investigating task-driven latent feasibility for nonconvex image modeling," *IEEE TIP*, 2020.
- [18] S. Dempe, N. Gadhi, and L. Laffhim, "Optimality conditions for pessimistic bilevel problems using convexificator," *Positivity*, pp. 1–19, 2020.
- [19] S. Dempe, *Bilevel optimization: theory, algorithms and applications*. TU Bergakademie Freiberg, Fakultät für Mathematik und Informatik, 2018.
- [20] R. Liu, J. Gao, J. Zhang, D. Meng, and Z. Lin, "Investigating bi-level optimization for learning and vision from a unified perspective: A survey and beyond," *arXiv preprint arXiv:2101.11517*, 2021.
- [21] M. J. Alves, C. H. Antunes, and J. P. Costa, "New concepts and an algorithm for multiobjective bilevel programming: optimistic, pessimistic and moderate solutions," *Operational Research*, pp. 1–34, 2019.
- [22] R. G. Jeroslow, "The polynomial hierarchy and a simple model for competitive analysis," *Mathematical programming*, 1985.
- [23] J. F. Bard and J. E. Falk, "An explicit solution to the multi-level programming problem," *Computers & Operations Research*, vol. 9, no. 1, pp. 77–100, 1982.
- [24] Z.-Q. Luo, J.-S. Pang, and D. Ralph, *Mathematical programs with equilibrium constraints*. Cambridge University Press, 1996.
- [25] D. Maclaurin, D. Duvenaud, and R. P. Adams, "Gradient-based hyperparameter optimization through reversible learning," in *ICML*, ser. JMLR Workshop and Conference Proceedings, 2015.
- [26] A. Shaban, C. Cheng, N. Hatch, and B. Boots, "Truncated back-propagation for bilevel optimization," in *AISTATS*, 2019.
- [27] F. Pedregosa, "Hyperparameter optimization with approximate gradient," in *ICML*, 2016.
- [28] J. Lorraine, P. Vicol, and D. Duvenaud, "Optimizing millions of hyperparameters by implicit differentiation," in *AISTATS*, 2020.
- [29] R. Liu, P. Mu, X. Yuan, S. Zeng, and J. Zhang, "A generic first-order algorithmic framework for bi-level programming beyond lower-level singleton," in *ICML*, 2020.
- [30] —, "A generic descent aggregation framework for gradient-based bi-level optimization," *arXiv preprint arXiv:2102.07976*, 2021.
- [31] J. V. Outrata, "On the numerical solution of a class of stackelberg problems," *ZOR-Methods and Models of Operations Research*, 1990.
- [32] J. J. Ye and D. L. Zhu, "Optimality conditions for bilevel programming problems," *Optimization*, 1995.
- [33] J. Bergstra and Y. Bengio, "Random search for hyper-parameter optimization," *JMLR*, 2012.
- [34] F. Hutter, H. H. Hoos, and K. Leyton-Brown, "Sequential model-based optimization for general algorithm configuration," in *International conference on learning and intelligent optimization*, 2011.

- [35] K. Ji, J. Yang, and Y. Liang, "Bilevel optimization: Nonasymptotic analysis and faster algorithms," *arXiv preprint arXiv:2010.07962v2*, 2020.
- [36] K. Ji and Y. Liang, "Lower bounds and accelerated algorithms for bilevel optimization," *arXiv preprint arXiv:2102.03926v2*, 2021.
- [37] A. V. Fiacco and G. P. McCormick, *Nonlinear programming: sequential unconstrained minimization techniques*. SIAM, 1990.
- [38] R. Grazzi, L. Franceschi, M. Pontil, and S. Salzo, "On the iteration complexity of hypergradient computation," in *ICML*, 2020.
- [39] L. S. Lasdon, "An efficient algorithm for minimizing barrier and penalty functions," *Mathematical Programming*, vol. 2, no. 1, pp. 65–106, 1972.
- [40] C. L. Byrne, "Alternating minimization as sequential unconstrained minimization: a survey," *Journal of Optimization Theory and Applications*, vol. 156, no. 3, pp. 554–566, 2013.
- [41] R. M. Freund, "Penalty and barrier methods for constrained optimization," *Lecture Notes, Massachusetts Institute of Technology*, 2004.
- [42] D. G. Luenberger, Y. Ye *et al.*, *Linear and nonlinear programming*. Springer, 1984, vol. 2.
- [43] D. Boukari and A. Fiacco, "Survey of penalty, exact-penalty and multiplier methods from 1968 to 1993," *Optimization*, vol. 32, no. 4, pp. 301–334, 1995.
- [44] A. Auslender, "Penalty and barrier methods: a unified framework," *SIAM Journal on Optimization*, vol. 10, no. 1, pp. 211–230, 1999.
- [45] J. F. Bonnans and A. Shapiro, *Perturbation analysis of optimization problems*. Springer Science & Business Media, 2013.
- [46] P. Borges, C. Sagastizábal, and M. Solodov, "A regularized smoothing method for fully parameterized convex problems with applications to convex and nonconvex two-stage stochastic programming," *Mathematical Programming*, 2020.
- [47] E. Grefenstette, B. Amos, D. Yarats, P. M. Htut, A. Molchanov, F. Meier, D. Kiela, K. Cho, and S. Chintala, "Generalized inner loop meta-learning," *arXiv preprint arXiv:1910.01727*, 2019.
- [48] H. Xiao, K. Rasul, and R. Vollgraf, "Fashion-mnist: a novel image dataset for benchmarking machine learning algorithms," *arXiv preprint arXiv:1708.07747*, 2017.
- [49] B. M. Lake, R. Salakhutdinov, and J. B. Tenenbaum, "Human-level concept learning through probabilistic program induction," *Science*, 2015.
- [50] I. Goodfellow, J. Pouget-Abadie, M. Mirza, B. Xu, D. Warde-Farley, S. Ozair, A. Courville, and Y. Bengio, "Generative adversarial nets," *Advances in neural information processing systems*, vol. 27, 2014.
- [51] M. Arjovsky, S. Chintala, and L. Bottou, "Wasserstein gan," 2017.